Journal of Medicinal Chemistry

Article

pubs.acs.org/jmc

Lead Optimization Studies on FimH Antagonists: Discovery of Potent and Orally Bioavailable Ortho-Substituted Biphenyl Mannosides

Zhenfu Han,[†] Jerome S. Pinkner,[‡] Bradley Ford,[§] Erik Chorell,[‡] Jan M. Crowley,[∥,⊥] Corinne K. Cusumano,[‡] Scott Campbell,[#] Jeffrey P. Henderson,[∥,⊥] Scott J. Hultgren,*[,‡,∥] and James W. Janetka*[,†,∥]

[†]Department of Biochemistry and Molecular Biophysics, [‡]Department of Molecular Microbiology, [§]Department of Pathology and Immunology, [∥]Center for Women's Infectious Disease Research, [⊥]Department of Internal Medicine, and [#]Department of Anesthesiology, Washington University School of Medicine, 660 S. Euclid Avenue, Saint Louis, Missouri 63110, United States

Supporting Information

ABSTRACT: Herein, we describe the X-ray structure-based design and optimization of biaryl mannoside FimH inhibitors. Diverse modifications to the biaryl ring to improve druglike physical and pharmacokinetic properties of mannosides were assessed for FimH binding affinity based on their effects on hemagglutination and biofilm formation along with direct FimH binding assays. Substitution on the mannoside phenyl ring ortho to the glycosidic bond results in large potency enhancements several-fold higher than those of corresponding unsubstituted matched pairs and can be rationalized from increased hydrophobic interactions with the FimH hydrophobic ridge (Ile13) or "tyrosine gate" (Tyr137 and Tyr48) also lined by Ile52. The lead mannosides have increased metabolic stability and oral bioavailability as determined from in vitro PAMPA predictive model of cellular permeability and in vivo pharmacokinetic studies in mice, thereby representing advanced preclinical candidates with promising potential as novel therapeutics for the clinical treatment and prevention of recurring urinary tract infections.

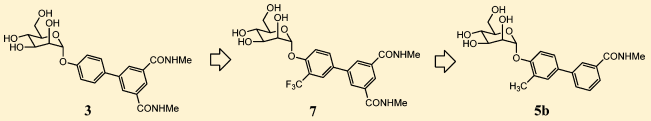

3	7	5b
HAI=370 nM	HAI=10 nM	HAI=60 nM
Biofilm IC_{50}=740 nM	Biofilm IC_{50}=43 nM	Biofilm IC_{50}=160 nM
PAMPA $LogP_e$=-4.51	PAMPA $LogP_e$=-6.27	PAMPA $LogP_e$=-3.89
Plasma (100 mpk; 6h)=0.01 μM	Plasma (50 mpk; 6h)=0.04 μM	Plasma (50 mpk; 6h)=0.10 μM
Urine (100 mpk; 6h)=4.85 μM	Urine (50 mpk; 6h)=0.89 μM	Urine (50 mpk; 6h)=4.37 μM

INTRODUCTION

FimH is a mannose-specific bacterial lectin located at the tip of type 1 pili, an adhesive fiber produced by uropathogenic *E. coli* (UPEC).[1] FimH is known to bind to mannosylated human uroplakins that coat the luminal surface of the bladder[2] and has also been shown to be involved in invasion of human bladder cells[3] and mast cells,[4] triggering apoptosis and exfoliation[5] and inducing elevated levels of cAMP.[6] Furthermore, FimH recognizes N-linked oligosaccharides on β1 and α3 integrins, which are expressed throughout the urothelium.[7] Murine uroplakin is highly homologous to human, and FimH has been shown to facilitate bacterial colonization and invasion of the bladder epithelium in murine models.[8] Internalized UPEC is exocytosed in a TLR-4 dependent process;[9] however, bacteria can escape into the host cell cytoplasm, where they are able to subvert expulsion and innate defenses by aggregating into biofilm-like intracellular bacterial communities (IBCs) in a FimH dependent process.[8b,c,10] Subsequently, UPEC species disperse from the IBC, escape into the bladder lumen, and reinitiate the process by binding and invading naive epithelial cells where they are able to establish quiescent intracellular reservoirs that can persist in a dormant state, tolerant to antibiotic therapy, and subsequently serve as seeds for recurrent infection.[11] In humans, the severity of UTI was increased and the immunological response was greater in children with infections caused by type 1 piliated UPEC strains and type 1 pilus expression has been shown to be essential for UTI in mouse models.[12] In addition, a recent study concluded that type 1 pili play an important role in human cystitis[13] and it has been reported that type 1 pili fulfill molecular Koch's postulates of microbial pathogenesis.[14] In agreement with these findings and in support of a role for FimH in humans, it has been shown that the fimH gene is under positive selection in human clinical isolates of UPEC.[8a,15] Aspects of the UPEC pathogenic cascade extensively characterized in a murine model of infection[8b,e,10] have been documented in samples from human clinical studies such as filamentation and IBC formation.[16]Targeted inhibitors of FimH adhesion which block both *E. coli* invasion and biofilm formation thus hold promising therapeutic potential as new antibacterials for the treatment of UTI and the prevention of recurrence.[17,18]

The discovery of simple D-mannose derivatives as inhibitors of bacterial adherence was first reported almost 3 decades ago,[19] but early mannosides showed only weak inhibition of bacterial adhesion. Consequently, the vast majority of research in this area has been focused on multivalent mannosides,[20] which have been pursued in an effort to improve binding avidity to type 1 pili, which can be expressed present in large numbers on a single bacterium (up to hundreds). While substantial progress has been made with this approach, these high molecular weight structures are not suitable for in vivo

Received: February 6, 2012
Published: March 26, 2012

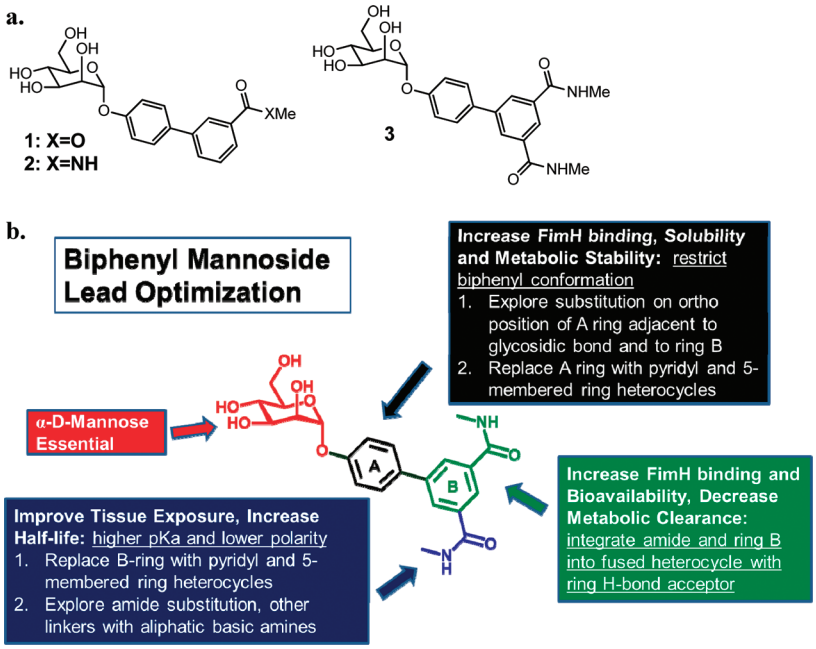

Figure 1. (a) Biphenyl mannoside FimH inhibitors with meta-substituted H-bond acceptors. (b) Lead optimization strategy of lead biphenyl mannoside **3** for increased FimH binding affinity, good druglike physical properties, and improved pharmacokinetics.

evaluation or clinical development as oral drugs. The recent X-ray crystal structures of D-mannose,[21] butyl mannoside,[22] and mannotriose[23] bound to FimH have enabled the rational structure-based design of tighter binding alkyl,[22] phenyl,[24] and biphenyl[25,26] mannoside FimH inhibitors. The urgency for developing new orally bioavailable FimH inhibitors[26] as a targeted strategy for the treatment of UTI alternative to broad spectrum antibiotics is reinforced by the rate of recurrence seen in these type of infections as well as increasing clinical resistance of UPEC to first line antibiotic treatments.[27]

RESULTS AND DISCUSSION

In an earlier study we reported the discovery of biphenyl mannosides **1**−**3** (Figure 1a) which make strong hydrophobic interactions to residues forming the outer "gate" of the FimH binding pocket. X-ray crystallographic data of compound **1** bound to FimH revealed both a key $\pi-\pi$ interaction of Tyr48 with the second phenyl ring of **1** and a tight H-bond between Arg98 and the ester carbonyl.[25] In this communication we describe the lead optimization of biphenyl mannoside **3** following the detailed strategy outlined in Figure 1b. Part of the plan was to improve FimH binding affinity through increased interactions with FimH using the structure of the FimH−**1** complex to guide our compound design. Directed by these structure−activity relationships (SARs), the final goal of optimization was to improve the metabolic stability, bioavailability, bladder tissue exposure, and in general the druglike properties of the mannosides through a multifaceted approach including heterocyclic replacements of both phenyl rings, ortho-substitution off each ring, and amide substitutions with higher pK_a moieties.

Ortho-Substituted Phenyl Mannosides. In addition to our work on mannoside FimH inhibitors Ernst[26] has subsequently described biphenyl mannosides as FimH antagonists and demonstrated that substitution with chlorine on the ortho-position of the phenyl ring directly attached to D-mannose resulted in a substantial increase in FimH inhibition. This key piece of SAR for phenyl mannosides was actually first observed in 1987 by Firon et al.[19] but has gone largely unnoticed until recently. As shown in Figure 2, Firon reported that *p*-nitro-*o*-chlorophenyl mannoside had a 10-fold increase in potency relative to *p*-nitrophenyl mannoside using a yeast hemagglutination assay, and later in 2006 Sperling et al. reported a 4-fold increase in activity from *o*-chlorine substitution on a different phenyl mannoside.[24] We also previously reported an 8-fold and 5-fold increase in activity, respectively, from ortho chlorine and nitrile substitution on phenyl mannoside but found that larger groups (e.g., phenyl) decreased potency.[25] Intrigued by these results from us and others, we were interested in elucidating the molecular basis for this increased potency derived from ortho substitution on the biphenyl ring.

Structure-Guided Design of Tight-Binding Ortho-Substituted Biaryl Mannosides. The structure of **1** bound to FimH suggested that the ortho-position of the ring attached to mannose is aimed at the Tyr137 residue at the ridge of FimH binding pocket and that improved hydrophobic contact and binding affinity to FimH could be achieved by substitution with small groups but would be sterically encumbered by larger groups such as an aryl ring.[25] Thus, we performed a matched pair analysis of monoester **1** compared to ortho-substituted analogues bearing halogen and small alkyl groups shown in Figure 3. The compounds were evaluated for their potency in the hemagglutination inhibition (HAI) assay,[28] and we discovered that all biphenyl ring substitutions yielded more potent inhibitors (Table 1). *o*-Cl mannoside **4b** had a HAI titer EC_{90} of 30 nM, which is more than 30-fold better than matched pair **1**, while the Me analogue **4c** was 8-fold more active (HAI titer EC_{90} = 120 nM). Substitution with CF_3 gave the most potent analogue **4d** with an HAI titer EC_{90} of 30 nM, whereas the OMe (**4e**) and F (**4a**) analogues showed smaller improvements in activity following the trend CF_3 > Cl = Me > OMe > F. These data suggest that increased hydrophobic contact with the tyrosine gate and Ile52 or with Ile13 at the opposite ridge of the mannose binding pocket could explain

dx.doi.org/10.1021/jm300165m | J. Med. Chem. 2012, 55, 3945−3959

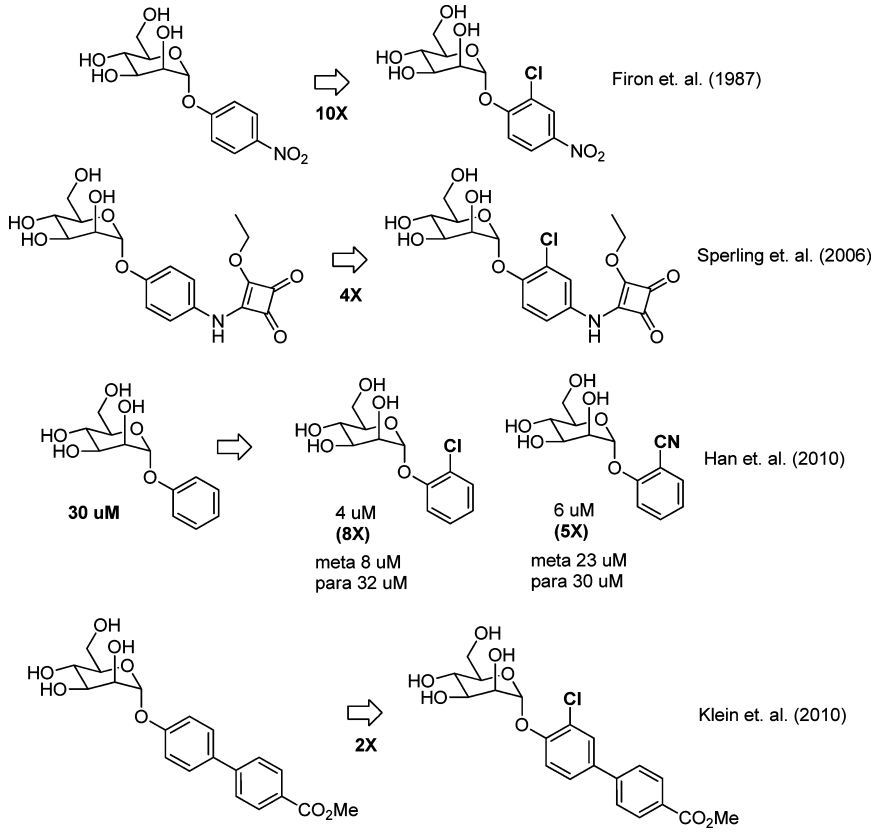

Figure 2. Potency enhancement from *o*-chloro substitution of phenyl mannosides.

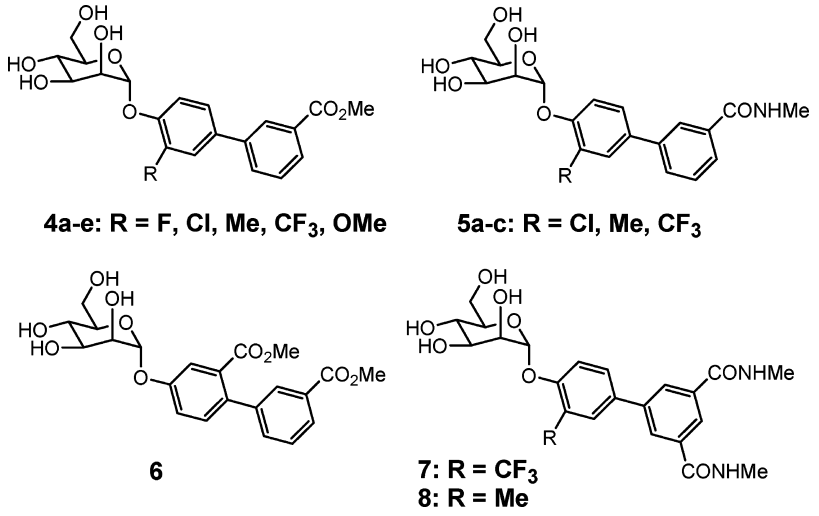

Figure 3. Substituted biphenyl mannosides.

this enhanced potency, since better activity correlates well with increased hydrophobicity as evidenced by the fact that fluoro analogue **4a** shows no improvement in activity relative to unsubstituted matched pair **1** and the trifluoromethyl analogue **4c**, which has the largest hydrophobic surface area, shows the highest activity. However, it is possible that the orientations of both phenyl rings are altered slightly[26] and are restricted to a conformation more conducive to improved FimH binding with Tyr137, Tyr48, Ile52, Ile13, and/or Arg98 residues.

The outcome of this preliminary study directed us to pursue analogues that were more metabolically stable and soluble than esters such as amides **5a**–**c** (Figure 3 and Table 1). A similar trend was observed (CF_3 > Me > Cl) with CF_3 amide **5c** having the best activity, but in this case the Me analogue **5b** showed better activity than the Cl analogue **5a**. We also explored analogues with substitution on the meta position, exemplified by ester **6**, which retains potency relative to **1** but did not lead to any enhancement. We next developed *o*-CF_3 **7** and Me **8** diamide matched pairs to original lead compound **3** which were exponentially more potent than any previously reported mannoside FimH inhibitors with an HAI titer EC_{90} of 8 and 16 nM, respectively. This unprecedented level of cellular

dx.doi.org/10.1021/jm300165m | *J. Med. Chem.* 2012, 55, 3945–3959

Table 1. Potency Enhancement and PAMPA Data from Ortho-Substitution of Biphenyl Mannosides

compd	HAI titer $EC_{>90}$ (μM)	biofilm prevention IC_{50} (μM)	MW (g/mol)	PSA	$CLogD_{7.4}$	PAMPA log P_e (cm^2/s)
1 (ester)	1.00	0.94	390.4	126	1.17	−5.42
4a (F)	0.75		408.4	126	1.00	
4b (Cl)	0.03	0.26	424.8	126	1.64	−4.29
4c (Me)	0.12	0.33	404.4	126	1.82	
4d (CF_3)	0.03	0.17	458.4	126	1.62	−3.91
4e (OMe)	0.19	0.89	420.4	135	0.47	
6 (*m*-CO_2Me)	1.0		448.4	152	0.93	−4.08
2 (amide)	0.50	1.35	389.4	128	0.28	
5a (Cl)	0.12	0.52	423.8	128	0.75	
5b (Me)	0.06	0.16	403.4	128	0.93	−3.89
5c (CF_3)	0.03	0.13	457.4	128	0.73	
3 (diamide)	0.37	0.74	446.4	158	0.71	−4.51
7 (CF_3)	0.01	0.043	514.5	158	1.15	−6.27
8 (Me)	0.02	0.073	460.5	158	1.35	−8.46

Scheme 1. Synthesis of Ortho-Substituted Biphenyl Mannosides[a]

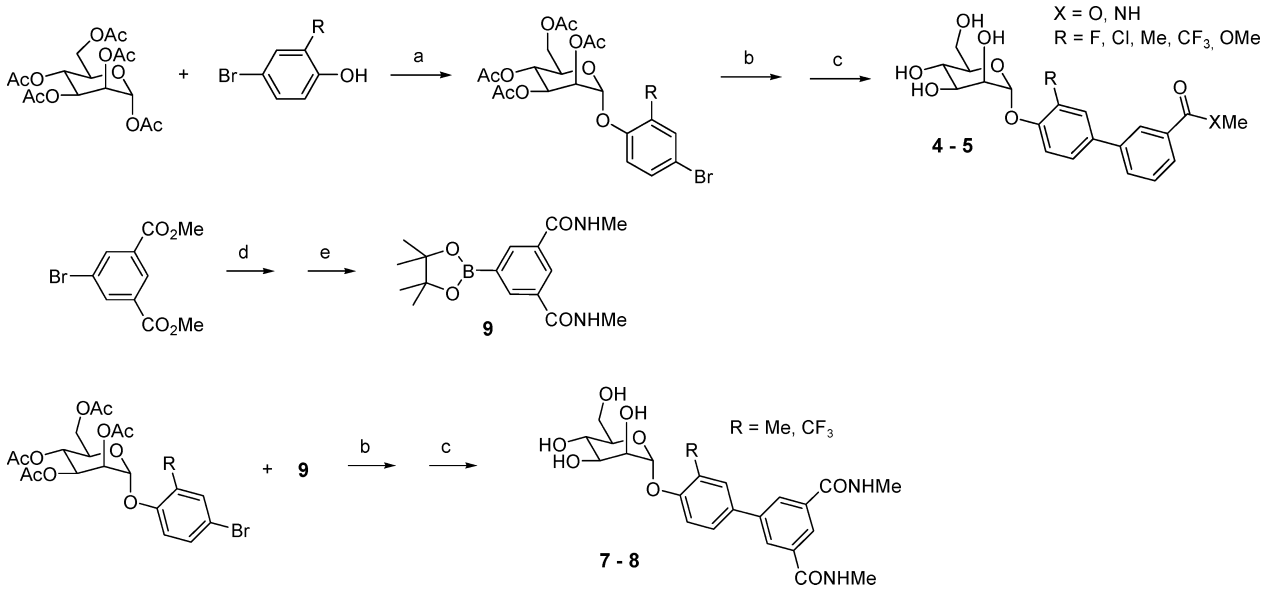

[a]Reagents and conditions: (a) BF_3−Et_2O, CH_2Cl_2, reflux; (b) 3-substituted phenylboronic acid derivatives, cat. $Pd(PPh_3)_4$, Cs_2CO_3, dioxane/water (5/1), 80 °C; (c) cat. MeONa, MeOH, rt; (d) $MeNH_2$/EtOH, rt; (e) bis(pinacolato)diboron, cat. $Pd(dppf)Cl_2$, KOAc, DMSO, 80 °C.

activity corresponds to a 200000-fold improvement over α-D-mannose and a 15000-fold improvement over an early reported inhibitor butyl-α-D-mannoside (HAI titer EC_{90} = 125 μM) and is 50-fold better than previous lead compound **3**.

The biofilm inhibition assay[17b,c,29] was utilized to test these mannosides' ability to prevent bacteria from forming IBCs, a critical pathogenic process in the development of UTIs. As shown in Table 1, the biofilm prevention IC_{50} values correlate quite well with the potencies determined by the HAI assay. Introduction of an ortho-substituent (e.g., methyl) to the biphenyl mannoside improved the biofilm activity by 8-fold from mannoside **2** (IC_{50} = 1.35 μM) to mannoside **5b** (IC_{50} = 0.16 μM). These data confirmed the mannoside's functional effect and activity on UPEC derived from FimH inhibition with a secondary assay. Biofilm IC_{50} values were utilized in conjunction with pharmacokinetic parameters as a key measure of the predicted lowest effective mannoside concentration in the urine required for efficacy in vivo, to be discussed vide infra.

Synthesis of Ortho-Substituted Biaryl Mannosides. Mannosides were synthesized by traditional Lewis acid mediated glycosylation of mannose pentaacetate by reaction with 2-substituted 4-bromophenols using BF_3 etherate (Scheme 1).[25,30] Suzuki cross-coupling with commercially available 3-substituted phenylboronic acid derivatives gave protected ortho-substituted 4′-biphenyl mannosides in excellent yields, and subsequent deprotection with NaOMe gave mannosides **4** and **5**. **6** was prepared following the procedure previously described.[25] Synthesis of diamides **7** and **8** followed a similar procedure but required the synthesis of 3,5-di-(*N*-methylaminocarbonyl)-phenylboronic acid pinacol ester **9**. Shown in Scheme 1, amidation of dimethyl 5-bromoisophthalate by reaction of methylamine in ethanol proceeded in quantitative yield to give *N,N*-dimethyl 5-bromoisophthalamide. Installation of the boronate ester was accomplished by Pd-mediated coupling with bis(pinacolato)diboron to give **9**.[31] Suzuki coupling and deprotection as before yielded compounds **7** and **8**.

dx.doi.org/10.1021/jm300165m | J. Med. Chem. 2012, 55, 3945−3959

Optimization of Mannosides for Increased Tissue Penetration and Half-Life. To help improve tissue penetration and identify mannosides with prolonged exposure in the bladder, we explored amide derivatives containing functional groups with higher pK_a (Table 2). Higher pK_a compounds containing basic moieties such as amines tend to have increased tissue penetration. Therefore, mannosides **10a–f** were prepared via standard 2-(7-aza-1*H*-benzotriazole-1-yl)-1,1,3,3-tetramethyluronium hexafluorophosphate (HATU) mediated coupling reaction of 4′-(α-D-mannopyranosyloxy)-biphenyl-3-carboxylic acid[25] with various amines. Unexpectedly, aminoethylamide **10b** showed a disappointing 6-fold drop in activity relative to methylamide **2**. However, hydroxyethylamide **10a** was equipotent to **2**. We also found that more hydrophobic tertiary amide piperazine analogues **10c** and **10d** had largely decreased potency (HAI EC_{90} = 4 μM). Interestingly, pyridylamides **10e** and **10f** showed slightly improved activity, most pronounced with 4-pyridyl derivative **10e**. While the reason for decreased potency of higher pK_a substituents is unclear, it is plausible that this effect could originate from charge−charge repulsion with Arg98 side chain at the edge of FimH binding pocket.

Table 2. Exploration of Amide Substitution with Increased pK_a

Compound	R	HAI Titer $EC_{>90}$ (μM)
10a	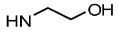	0.50
10b	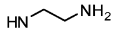	3.0
10c		4.0
10d		4.0
10e		0.25
10f		0.37

Exploration of Heterocyclic Mannosides for Improved Pharmacokinetics. We next pursued heterocyclic replacements of the terminal biphenyl ring as an alternative approach to improve the druglike properties of lead mannosides and potentially decrease the metabolic clearance. In our target compounds we retained the key H-bond donor to Arg98 of FimH, so we could directly compare the effects of heterocyclic ring replacement. In order to synthesize a library of heterocycles in a divergent fashion, we developed a new Suzuki synthesis using a 4-mannopyranosyloxyphenyl boronate intermediate **11**[32] in place of 4-bromophenyl α-D-mannoside. Only a limited number of heteroaryl boronates are commercially available, and this new methodology allows for the use of more readily obtainable heteroaryl bromides as coupling partners. All heteroaryl bromides used in Table 3 were commercially available with reasonable prices except bromothiophene derivatives **16** and **17** (Scheme 2). **16** was prepared via Curtius reaction by first treatment of 5-bromothiophene-3-carboxylic acid with diphenylphosphorylazide (DPPA) to form isocyanate intermediate, then quenching with ammonia. **17** was synthesized according to previous method.[33] As shown in Scheme 2, Starting from 4-bromophenyl-α-D-mannoside, bis(pinacolato)-diboron, and Pd(dppf)Cl_2 in DMSO, intermediate **11** was prepared in good yield. Suzuki cross-coupling of **11** with various aryl bromides followed by acetyl deprotection gave target compounds. Compounds synthesized, shown in Table 3, include pyridyl esters **12a** and **12b** which showed excellent activity in the HAI titer with improvement over phenyl ester **1**. Furthermore, ring replacement with a thiophene urea carboxylate led to dramatic advancements in FimH activity as exemplified by compound **13a** which has HAI EC_{90} = 16 nM. In order to ascertain whether the carboxylate ester group or urea was responsible for this large increase in potency, we synthesized ester **13b** and urea **13c** to discover that the enhancement results from a combined effect of both functionals, since **13b** and **13c** have much decreased activity. It is unknown why there is a synergistic effect from the compound with both urea and carboxylate, but from previous work on thiophene carboxamide ureas[33b] we have shown that an intramolecular H-bond exists between the internal NH of the urea and the carbonyl of the ester. This conformational

Table 3. Heterocyclic Modifications to Biphenyl Ring for Improving Druglike Properties

Compound	R	HAI Titer $EC_{>90}$ (μM)
12a	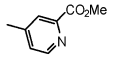	0.50
12b	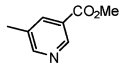	0.19
13a	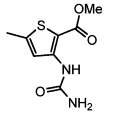	0.02
13b	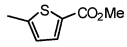	1.0
13c	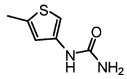	1.0
13d	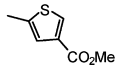	2.0
14a	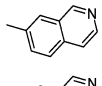	0.75
14b	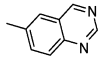	0.38
15a		0.25
15b	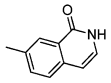	0.10

dx.doi.org/10.1021/jm300165m | J. Med. Chem. 2012, 55, 3945−3959

Scheme 2. Synthesis of Heterocyclic Mannosides[a]

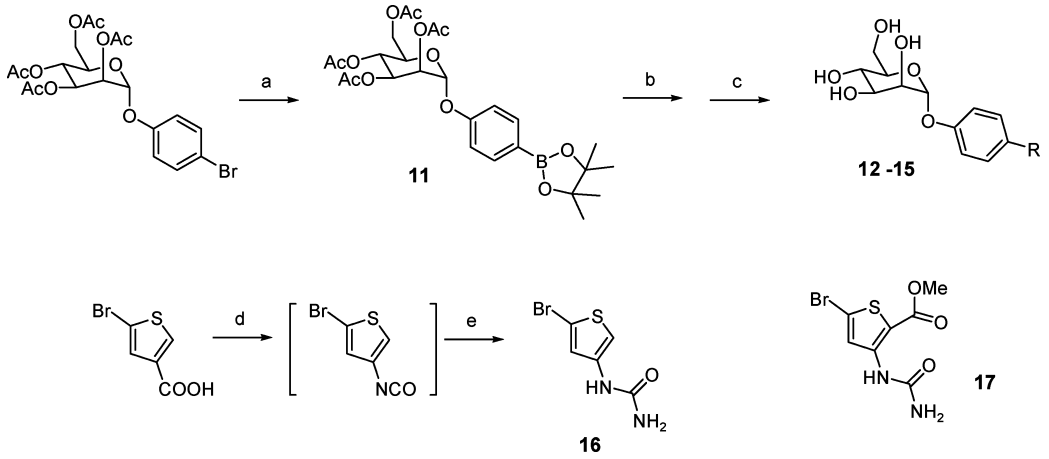

[a]Reagents and conditions: (a) bis(pinacolato)diboron, cat. $Pd(dppf)Cl_2$, KOAc, DMSO, 80 °C; (b) heteroaryl bromide derivatives, cat. $Pd(PPh_3)_4$, Cs_2CO_3, dioxane/water (5/1), 80 °C; (c) cat. MeONa, MeOH, rt; (d) DPPA, $^iPr_2NEt$, dioxane, 85 °C; (e) NH_3/dioxane (0.5 M), rt.

restriction might enhance binding entropically to FimH, likely from the urea carbonyl. We also pursued several fused rings such as isoquinoline derivatives **14** and **15** to examine the effects of isosteric replacement for the arylcarbonyl H-bond acceptor,[25] where the heterocyclic ring nitrogen is designed to accept a H-bond from the FimH Arg98 side chain. The promising HAI assay results for **14a**,**b** to **15a**,**b** clearly provide much evidence that the orientation of the C═N in **15a** or C═O in **15b** is likely the same as the conformation of C═O of mannoside **1** in the crystal structure of FimH−mannoside **1**,[25] bringing the potency up by as much as 10-fold over mannoside **1**.

Direct FimH Binding Studies and Pharmacophore Model for Mannosides. In order to better understand how the excellent potency in cell-based HAI and biofilm assays is correlated with FimH binding by biaryl mannosides and to more precisely select the best lead compounds for in vivo pharmacokinetic (PK) studies, we have developed a biolayer interferometry method to directly measure the binding affinities (K_d) of FimH inhibitors. As shown in Table 4, earlier mannosides **19**−**33**[25] showing moderate potency in the HAI assay had K_d values as low as 1−10 nM. Strikingly, for compounds **1** and **2**, K_d values were in the picomolar range. For mannosides **5**, **7**, and **8**, however, K_d could not be calculated because the off-rates were too low to measure. In order to overcome this obstacle, we utilized differential scanning fluorimetry (DSF) to rank the high-affinity mannosides. DSF measures the melting temperature change of protein when binding to small molecules.[34] Melting temperature shifts are proportional to the free energy of binding, and melting temperatures increase even as ligand concentration exceeds the K_d.[35] As illustrated in Table 4 and Figure 4, the melting temperature of FimH without mannoside was about 60 °C and rose to between 68 and 74 °C when binding to mannosides **19**−**33** of moderate potency. With tight binding mannosides **5b**, **7**, **8** the melting temperature of FimH ranged from 74 to 76 °C, suggesting that improved mannosides likely bind FimH with low picomolar affinity. Figure 4 illustrates that DSF ranks mannosides in a similar fashion to the HAI assay except for **5c** and **25**, demonstrating that this is a general and reliable method to qualitatively rank FimH-mannoside binding when K_d values span many orders of magnitude. Thus, these direct FimH binding studies solidified that the high potencies stemming from mannosides **5b**, **7**, **8** are derived directly from extremely tight binding to the FimH lectin and not other nonspecific effects from the cell assays.

Although thus far we have not yet been successful in aquiring an X-ray structure of one of these new ortho-substituted mannosides bound to FimH, we have generated an electrostatic surface with the most potent mannoside **7** docked to FimH shown in Figure 5. The large boost in binding affinity to FimH can be attributed to the fact that in our model the ortho trifluoromethyl group is oriented directly at Ile13, resulting in a very strong hydrophobic interaction with FimH. The added hydrophobicity encompassed by the fluorine atoms in mannoside **7** results in further augmented binding to FimH relative to ortho methyl mannoside **8**. X-ray crystallographic studies are aggressively being pursued to confirm this proposed hypothetical model and to elucidate potential other reasons for the improved binding affinity with regard to either compound or FimH conformation.

Stability and Elimination Kinetics of Mannosides. We recently reported that mannoside **3** shows efficacy in vivo[36] in the treatment and prevention of established UTIs in mice when dosed orally, but the compound displayed some metabolic instability from hydrolysis of the glycosidic bond (Figure 6a) and very rapid elimination kinetics to the urine partly due to its low CLogD (Table 1). While renal clearance is an attractive feature for UTI therapy, we still wanted to develop improved mannosides encompassing lower clearance rates as well as increased oral bioavailability and bladder tissue permeability. In order to have a general idea of the elimination rate of mannoside **3**, PK studies of its urinary clearance were conducted in mice (Figure 6b). These experiments demonstrated that the lower oral dosing of 20 mg/kg was unlikely to maintain effective concentrations (as determined by biofilm IC_{50}) because of rapid clearance. Maintenance of mannoside **3** levels above the minimal effective level of 0.74 μM (based on the biofilm prevention IC_{50} in Table 1) during in an 8 h period required a larger, 100 mg/kg dose. During the PK study, we detected a small amount of a phenolic biphenyl metabolite (R) (Figure 6a) in the urine, indicating that some glycoside bond hydrolysis takes place upon oral dosing. Urine levels of the R group were unchanged from the 100 and 200 mg/kg doses,

dx.doi.org/10.1021/jm300165m | J. Med. Chem. 2012, 55, 3945−3959

Table 4. Results of Octet Assay and DSF Assay[a]

Compound	Structure of R	HAI Titer $EC_{>90}$ (μM)	Octet K_d (nM)	DSF Melting Temp. (°C)
7	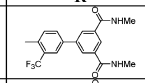	0.008	N.D.*	76.15
8	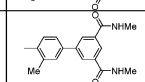	0.016	N.D.*	75.76
5c	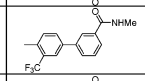	0.032	N.D.*	72.29
5b	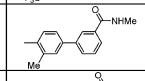	0.060	N.D.*	74.46
18[25]	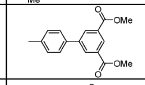	0.150	N.D.*	72.53
10f	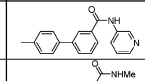	0.375	N.D.*	72.53
3	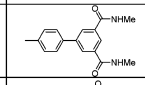	0.375	0.14	74.39
12a	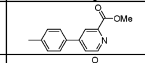	0.500	N.D.*	73.68
2	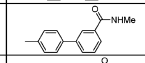	0.500	0.01	73.38
19[25]	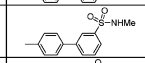	1.000	0.49	72.05
1	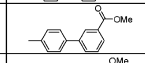	1.000	0.08	73.39
20[25]	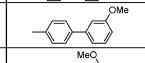	1.500	1.25	71.77
21[25]	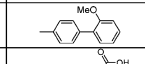	2.000	N.D.*	70.72
22[25]	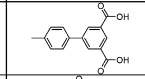	2.000	14.5	72.39
23[25]	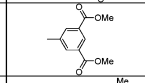	2.000	3.45	73.25
24[25]	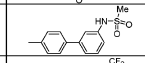	2.000	2.00	70.90
25[25]	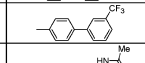	2.000	1.56	68.32
26[25]	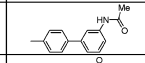	2.000	1.14	72.30
27[25]	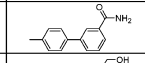	2.000	1.00	71.69
28[25]		3.000	2.61	71.16
29[25]	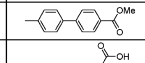	4.000	3.99	68.69
30[25]	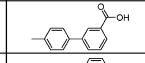	4.000	2.21	70.93
31[25]	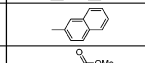	6.000	2.72	70.75
32[25]	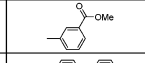	6.000	2.72	70.75
33[25]		8.000	3.00	71.17
Phenyl-α-D-mannoside	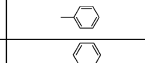	30.000	N.D.*	68.93
34[25]	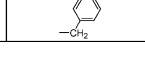	60.000	43.66	68.11

[a](*) N.D. = not determined.

suggesting that metabolism by glycoside bond hydrolysis is saturated between the 20 and 100 mg/kg doses (Figure 6b).

In Vitro Parallel Artificial Membrane Permeability Assay (PAMPA). The low log *D* of polyhydroxylated sugar-based

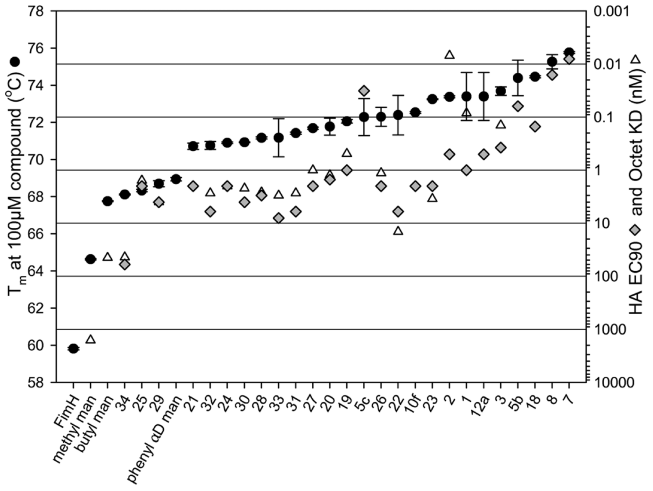

Figure 4. Curves of HAI, Octet, and DSF assay results.

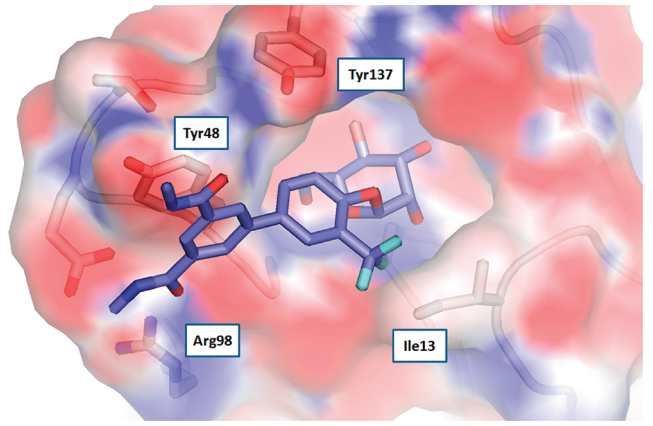

Figure 5. Proposed model of mannoside **7** bound to FimH calculated with APBS (Adaptive Poisson−Boltzmann Solver) software using PDB code 3MCY.[25]

mannosides and other carbohydrate-derived compounds[37] can limit their ability to cross cell membranes in the absence of active transport mechanisms, and so increasing their hydrophobicity is one strategy to help improve cell permeability and oral bioavailability of this class of molecules. The ortho-substituted mannosides described above were designed for increased hydrophobic contact with FimH but also in part to increase the log *D* and were predicted to improve the solubility, oral bioavailability, and bladder tissue penetration relative to starting mannosides **1**−**3**. It was anticipated that the newly designed inhibitors would also have increased metabolic stability via protection of the glycosidic bond from acidic hydrolysis in the gut and enzymatic hydrolysis by α-mannosidases in blood and tissues. In order to test these hypotheses experimentally, we used the PAMPA. PAMPA is commonly used as an in vitro model of passive, transcellular permeability to predict oral bioavailability for drug candidates.[38] We tested the most potent biphenyl mannosides in this model for prioritizing compounds to evaluate further in animal PK and efficacy studies. Shown in Table 1, compound **5b** with log P_e of −3.89 cm^2/s proved to have the highest oral absorption, while the most potent mannosides (determined by HAI assay) **7** and **8** with log P_e of −6.27 and −8.46 cm^2/s exhibited significantly lower oral bioavailability.

dx.doi.org/10.1021/jm300165m | J. Med. Chem. 2012, 55, 3945−3959

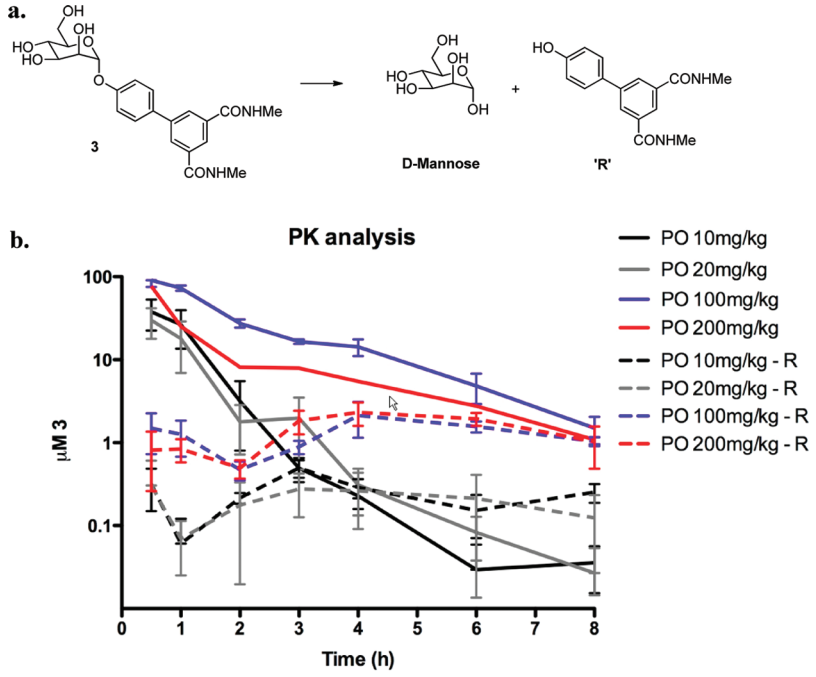

Figure 6. (a) Metabolic lability of the mannoside **3** glycosidic bond from hydrolysis to mannose and biphenol. (b) Elimination kinetics and clearance of mannoside **3** and biphenol (R) hydrolysis product in mouse urine.

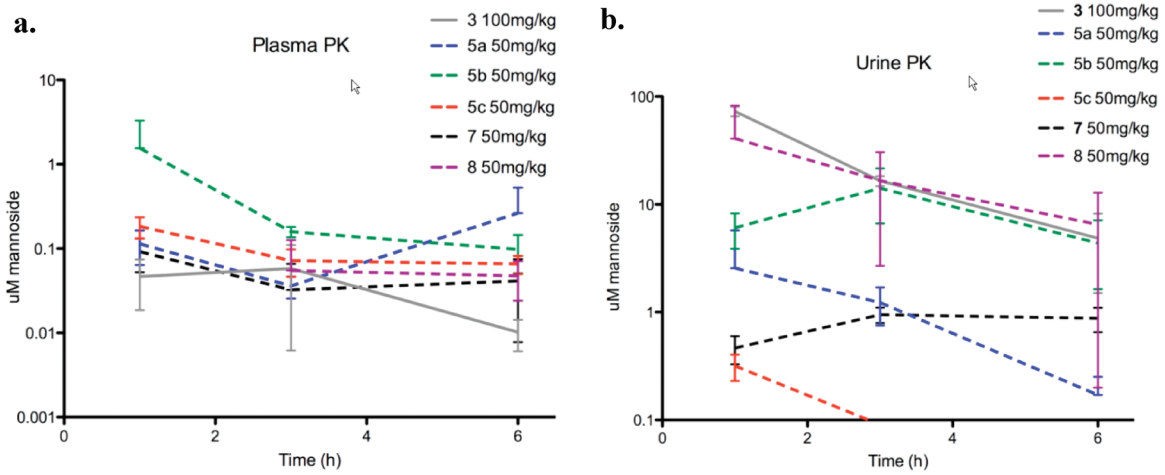

Figure 7. (a) Plasma pharmacokinetics of optimized ortho-substituted mannosides **5a**–**c**, **7**, **8** and mannoside **3**. (b) Elimination clearance kinetics of optimized ortho-substituted mannosides **5a**–**c**, **7**, **8** and mannoside **3** in urine.

In Vivo Pharmacokinetic Studies of Ortho-Substituted Biphenyl Mannoside Inhibitors. On the basis of these results, oral PK studies were performed in mice to assess any improvements in the PK of these ortho-substituted mannosides. Compounds were dosed at 50 mg/kg, and plasma and urine samples were taken at 30 min and 1, 2, 3, 4, 6 h after dosing. As demonstrated in Figure 7, a generally 10-fold higher mannoside concentration was observed in urine (Figure 7b) compared to plasma (Figure 7a), indicating a high clearance rate for these mannosides, which in this case aids in clearing uropathogens on the bladder surface. We found that compounds **8** and **5b** consistently maintain a high level of concentration in both urine and plasma, which is well above the predicted minimum effective concentration within a 6 h period. While 100 mg/kg dosing of mannoside **3** was required to achieve effective mannoside concentrations, only 50 mg/kg dosing of mannoside **5b** was required, permitting a much larger therapeutic window for treatment. Taken together with PAMPA results, high oral bioavailability and in vivo efficacy in recently reported animal studies[36] support mannoside **5b** as the most promising therapeutic candidate for UTI treatment/prevention.

CONCLUSIONS

Using a combination of traditional ligand-based and X-ray structure-guided approaches with SAR driven by cell-based hemagglutination and biofilm assays in combination with direct FimH binding assays, we have identified a diverse array of biaryl mannoside FimH inhibitors that exhibit binding affinities into the picomolar range. While we found the most potent mannoside **7** with respect to FimH binding affinity and activity in cell assays contains an *o*-trifluoromethyl group off the phenyl ring adjacent to the mannose ring group, the most promising inhibitor from in vivo studies is the *o*-methyl analogue **8** showing prolonged compound exposure in plasma and urine

dx.doi.org/10.1021/jm300165m | *J. Med. Chem.* 2012, 55, 3945–3959

PK studies. We rationalize the large FimH binding affinity improvement. We have also discovered a variety of heterocyclic biaryl mannosides that either retain or improve FimH binding activity. The novel inhibitors of UPEC type 1 mediated bacterial adhesion reported herein show unprecedented activity in hemagglutination and biofilm in vitro assays in addition to desirable PK properties in vivo. Further optimization of lead mannosides is currently being focused on the identification of mannose modifications with reduced sugar-like character.[39] Biaryl mannosides have high potential as innovative therapeutics for the clinical treatment and prevention of UTIs. This report describes the most potent mannoside FimH inhibitors to date that display good oral bioavailability and druglike properties in vivo. The unique mechanism of action of targeting the pilus tip adhesin, FimH, circumvents the conventional requirement for drug penetration of the outer membrane and the potential for development of resistance by porin mutations, efflux, or degradative enzymes, all mechanisms that promote resistance to antibiotics. Current efforts are directed at the selection of one or more clinical candidate drugs through rigorous preclinical evaluation in several models of recurrent UTI with antibiotic resistant forms of UPEC. These preclinical models will facilitate further optimization of current lead compounds to clinical candidate drugs which promise to provide a new and more selective therapy to treat and prevent chronic and recurrent urinary tract infections for which there is currently no effective treatment. Furthermore, since mannoside FimH inhibitors function outside the cell and are not cytotoxic to bacteria in contrast to all commonly prescribed antibiotics susceptible to resistance, this innovative therapeutic strategy could dramatically reduce resistant forms of uropathogenic *E. coli*.

EXPERIMENTAL SECTION

General Synthesis, Purification, and Analytical Chemistry Procedures. Starting materials, reagents, and solvents were purchased from commercial vendors unless otherwise noted. ^{1}H NMR spectra were measured on a Varian 300 MHz NMR instrument. The chemical shifts were reported as δ ppm relative to TMS using residual solvent peak as the reference unless otherwise noted. The following abbreviations were used to express the multiplicities: s = singlet; d = doublet; t = triplet; q = quartet; m = multiplet; br = broad. High-performance liquid chromatography (HPLC) was carried out on Gilson GX-281 using Waters C18 5 μm, 4.6mm × 50 mm and Waters Prep C18 5 μm, 19 mm × 150 mm reverse phase columns, eluting with a gradient system of 5:95 to 95:5 acetonitrile/water with a buffer consisting of 0.05% TFA. Mass spectrometry (MS) was performed on an HPLC/MSD instrument using electrospray ionization (ESI) for detection. All reactions were monitored by thin layer chromatography (TLC) carried out on Merck silica gel plates (0.25 mm thick, 60F254), visualized by using UV (254 nm) or dyes such as $KMnO_4$, *p*-anisaldehyde, and CAM. Silica gel chromatography was carried out on a Teledyne ISCO CombiFlash purification system using prepacked silica gel columns (12−330 g sizes). All compounds used for biological assays are greater than 95% pure based on NMR and HPLC by absorbance at 220 and 254 nm wavelengths.

Procedures for the Preparation of Biphenyl Mannoside Derivatives through Suzuki Coupling Reaction with Bromophenyl Mannoside Derivatives as Intermediates: 4′-(α-D-Mannopyranosyloxy)-*N*,3′-dimethylbiphenyl-3-carboxamide (5b). 4-Bromo-2-methylphenyl 2,3,4,6-Tetra-*O*-acetyl-α-D-mannopyranoside. Under nitrogen atmosphere and at room temperature, boron trifluoride diethyl etherate (3.41 g, 24 mmol) was added dropwise into a solution of α-D-mannose pentaacetate (3.12 g, 8 mmol) and 4-bromo-2-methylphenol (2.99 g, 16 mmol) in 100 mL of anhydrous CH_2Cl_2. After a few minutes the mixture was heated to reflux and kept stirring for 45 h. The reaction was then quenched with water, and extraction was with CH_2Cl_2. The CH_2Cl_2 layer was collected, dried with Na_2SO_4, and concentrated. The resulting residue was purified by silica gel chromatography with hexane/ethyl acetate combinations as eluent, giving 4-bromo-2-methylphenyl 2,3,4,6-tetra-*O*-acetyl-α-D-mannopyranoside (3.22 g) in 77% yield. ^{1}H NMR (300 MHz, chloroform-*d*) δ ppm 7.18−7.38 (m, 2H), 6.97 (d, *J* = 8.79 Hz, 1H), 5.50−5.59 (m, 1H), 5.43−5.50 (m, 2H), 5.32−5.42 (m, 1H), 4.28 (dd, *J* = 5.63, 12.50 Hz, 1H), 3.99−4.15 (m, 2H), 2.27 (s, 3H), 2.20 (s, 3H), 2.02−2.11 (three singlets, 9H). MS (ESI): found $[M + Na]^+$, 539.0.

4′-(α-D-Mannopyranosyloxy)-*N*,3′-dimethylbiphenyl-3-carboxamide (5b). Under nitrogen atmosphere, a mixture of 4-bromo-2-methylphenyl 2,3,4,6-tetra-*O*-acetyl-α-D-mannopyranoside (0.517 g, 1 mmol), 3-(*N*-methylaminocarbonyl)phenylboronic acid pinacol ester (0.392 g, 1.5 mmol), cesium carbonate (0.977 g, 3 mmol), and tetrakis-(triphenylphosphine)palladium (0.116 g, 0.1 mmol) in dioxane/water (15 mL/3 mL) was heated at 80 °C with stirring for 1 h under a nitrogen atmosphere. After cooling to room temperature, the mixture was filtered through silica gel column to remove the metal catalyst and salts with hexane/ethyl acetate combinations as eluent. The filtrate was concentrated and then dried in vacuo. The residue was diluted with 15 mL of methanol containing a catalytic amount of sodium methoxide (0.02 M), and the mixture was stirred at room temperature overnight. H^+ exchange resin (DOWEX 50WX4-100) was added to neutralize the mixture. The resin was filtered off, and the filtrate was concentrated. The resulting residue was purified by silica gel chromatography with CH_2Cl_2/MeOH combinations as eluent, giving the title compound (0.260 g) in 64% yield for two steps. ^{1}H NMR (300 MHz, methanol-d_4) δ ppm 7.94 (t, *J* = 1.65 Hz, 1H), 7.57−7.72 (m, 2H), 7.33−7.50 (m, 3H), 7.23 (d, *J* = 8.52 Hz, 1H), 5.48 (d, *J* = 1.92 Hz, 1H), 4.00 (dd, *J* = 1.79, 3.43 Hz, 1H), 3.83−3.94 (m, 1H), 3.60−3.76 (m, 3H), 3.46−3.58 (m, 1H), 2.87 (s, 3H), 2.24 (s, 3H). MS (ESI): found $[M + H]^+$, 404.2.

Methyl 3′-Fluoro-4′-(α-D-mannopyranosyloxy)biphenyl-3-carboxylate (4a). 4-Bromo-2-fluorophenyl 2,3,4,6-Tetra-*O*-acetyl-α-D-mannopyranoside. 4-Bromo-2-fluorophenyl 2,3,4,6-tetra-*O*-acetyl-α-D-mannopyranoside was prepared using the same procedure as for 4-bromo-2-methylphenyl 2,3,4,6-tetra-*O*-acetyl-α-D-mannopyranoside in the synthesis of **5b**. Yield: 25%. ^{1}H NMR (300 MHz, chloroform-*d*) δ ppm 7.30 (dd, *J* = 2.34, 10.03 Hz, 1H), 7.21 (td, *J* = 1.79, 8.79 Hz, 1H), 7.08 (t, *J* = 8.52 Hz, 1H), 5.48−5.58 (m, 2H), 5.46 (d, *J* = 1.65 Hz, 1H), 5.31−5.41 (m, 1H), 4.23−4.31 (m, 1H), 4.13−4.22 (m, 1H), 4.05−4.13 (m, 1H), 2.20 (s, 3H), 2.02−2.08 (three singlets, 9H). MS (ESI): found $[M + Na]^+$, 543.0.

Methyl 3′-Fluoro-4′-(α-D-mannopyranosyloxy)biphenyl-3-carboxylate (4a). 4a was prepared using the same procedure as for **5b** with 4-bromo-2-fluorophenyl 2,3,4,6-tetra-*O*-acetyl-α-D-mannopyranoside and 3-methoxycarbonylphenyl boronic acid as the reactants. Yield: 66%. ^{1}H NMR (300 MHz, methanol-d_4) δ ppm 8.21 (t, *J* = 1.65 Hz, 1H), 7.99 (td, *J* = 1.44, 7.83 Hz, 1H), 7.84 (ddd, *J* = 1.10, 1.92, 7.69 Hz, 1H), 7.35−7.62 (m, 4H), 5.55 (d, *J* = 1.92 Hz, 1H), 4.10 (dd, *J* = 1.79, 3.43 Hz, 1H), 3.94 (s, 3H), 3.86−4.00 (m, 1H), 3.59−3.86 (m, 4H). MS (ESI): found $[M + Na]^+$, 431.1.

Methyl 3′-Chloro-4′-(α-D-mannopyranosyloxy)biphenyl-3-carboxylate (4b). 4-Bromo-2-chlorophenyl 2,3,4,6-Tetra-*O*-acetyl-α-D-mannopyranoside. 4-Bromo-2-chlorophenyl 2,3,4,6-tetra-*O*-acetyl-α-D-mannopyranoside was prepared using the same procedure as for 4-bromo-2-methylphenyl 2,3,4,6-tetra-*O*-acetyl-α-D-mannopyranoside in the synthesis of **5b**. Yield: 46%. ^{1}H NMR (300 MHz, chloroform-*d*) δ ppm 7.55 (d, *J* = 2.47 Hz, 1H), 7.33 (dd, *J* = 2.47, 8.79 Hz, 1H), 7.06 (d, *J* = 8.79 Hz, 1H), 5.58 (dd, *J* = 3.02, 10.16 Hz, 1H), 5.52 (s, 1H), 5.49−5.54 (m, 1H), 5.33−5.42 (m, 1H), 4.22−4.32 (m, 1H), 4.04−4.17 (m, 2H), 2.21 (s, 3H), 2.07 (s, 3H), 2.05 (s, 3H), 2.04 (s, 3H). MS (ESI): found $[M + Na]^+$, 561.0 .

Methyl 3′-Chloro-4′-(α-D-mannopyranosyloxy)biphenyl-3-carboxylate (4b). 4b was prepared using the same procedure as for **5b** with 4-bromo-2-chlorophenyl 2,3,4,6-tetra-*O*-acetyl-α-D-mannopyranoside and 3-methoxycarbonylphenyl boronic acid as the reactants. It was further purified by HPLC (C18, 15 mm × 150 mm column; eluent, acetonitrile/water (0.1% TFA)). Yield: 43%. ^{1}H NMR (300 MHz, methanol-d_4) δ ppm 3.59−3.71 (m, 1 H), 3.71−3.85 (m, 3 H), 3.94 (s, 3 H), 4.01 (dd, *J* = 9.34, 3.30 Hz, 1 H), 4.12 (dd, *J* = 3.30, 1.92 Hz, 1 H),

dx.doi.org/10.1021/jm300165m | J. Med. Chem. 2012, 55, 3945−3959

5.61 (d, J = 1.65 Hz, 1 H), 7.40−7.49 (m, 1 H), 7.49−7.62 (m, 2 H), 7.68 (d, J = 2.20 Hz, 1 H), 7.82 (ddd, J = 7.76, 1.85, 1.10 Hz, 1 H), 7.98 (dt, J = 7.83, 1.30 Hz, 1 H), 8.14−8.25 (m, 1 H). MS (ESI): found $[M + H]^+$, 425.1.

Methyl 4′-(α-D-Mannopyranosyloxy)-3′-methylbiphenyl-3-carboxylate (4c). **4c** was prepared using the same procedure as for **5b** with 4-bromo-2-methylphenyl 2,3,4,6-tetra-*O*-acetyl-α-D-mannopyranoside and 3-methoxycarbonylphenyl boronic acid as the reactants. Yield: 54%. ^{1}H NMR (300 MHz, methanol-d_4) δ ppm 8.20 (t, J = 1.51 Hz, 1H), 7.94 (td, J = 1.41, 7.90 Hz, 1H), 7.77−7.87 (m, 1H), 7.52 (t, J = 7.55 Hz, 1H), 7.39−7.48 (m, 2H), 7.27−7.38 (m, 1H), 5.56 (d, J = 1.65 Hz, 1H), 4.08 (dd, J = 1.92, 3.30 Hz, 1H), 3.94−4.01 (m, 1H), 3.90−3.94 (m, 3H), 3.68−3.83 (m, 3H), 3.55−3.65 (m, 1H), 2.31 (s, 3H). MS (ESI): found $[M + Na]^+$, 427.1.

Methyl 4′-(α-D-Mannopyranosyloxy)-3′-(trifluoromethyl)-biphenyl-3-carboxylate (4d). 4-Bromo-2-(trifluoromethyl)-phenyl 2,3,4,6-Tetra-*O*-acetyl-α-D-mannopyranoside. 4-Bromo-2-(trifluoromethyl)phenyl 2,3,4,6-tetra-*O*-acetyl-α-D-mannopyranoside was prepared using the same procedure as for 4-bromo-2-methylphenyl 2,3,4,6-tetra-*O*-acetyl-α-D-mannopyranoside in the synthesis of **5b**. Yield: 54%. ^{1}H NMR (300 MHz, chloroform-*d*) δ ppm 7.74 (d, J = 2.20 Hz, 1H), 7.61 (dd, J = 2.33, 8.93 Hz, 1H), 7.15 (d, J = 8.79 Hz, 1H), 5.61 (d, J = 1.92 Hz, 1H), 5.48−5.56 (m, 1H), 5.33−5.48 (m, 2H), 4.21−4.34 (m, 1H), 3.97−4.14 (m, 2H), 2.21 (s, 3H), 1.99−2.12 (three singlets, 9H). MS (ESI): found $[M + Na]^+$, 593.0.

Methyl 4′-(α-D-Mannopyranosyloxy)-3′-(trifluoromethyl)-biphenyl-3-carboxylate (4d). **4d** was prepared using the same procedure as for **5b** with 4-bromo-2-(trifluoromethyl)phenyl 2,3,4,6-tetra-*O*-acetyl-α-D-mannopyranoside and 3-methoxycarbonylphenyl boronic acid as the reactants. Yield: 53%. ^{1}H NMR (300 MHz, methanol-d_4) δ ppm 8.23 (t, J = 1.51 Hz, 1H), 8.01 (td, J = 1.37, 7.69 Hz, 1H), 7.80−7.93 (m, 3H), 7.52−7.67 (m, 2H), 5.66 (d, J = 1.65 Hz, 1H), 4.07 (dd, J = 1.79, 3.43 Hz, 1H), 3.95 (s, 3H), 3.90−4.00 (m, 1H), 3.66−3.87 (m, 3H), 3.52−3.66 (m, 1H). MS (ESI): found $[M + Na]^+$, 481.0.

Methyl 4′-(α-D-Mannopyranosyloxy)-3′-methoxybiphenyl-3-carboxylate (4e). **4e** was prepared using the same procedure as for **5b**. In the first step of glycosidation reaction 4-bromo-2-methoxyphenol was used as glycosidation acceptor, and in the second step of Suzuki coupling reaction 3-methoxycarbonylphenylboronic acid was used instead. All intermediates were directly taken to the next step reaction without further purification. **4e** was further purified by HPLC (C18, 15 mm × 150 mm column; eluent, acetonitrile/water (0.1% TFA)). Yield: 3%. ^{1}H NMR (300 MHz, methanol-d_4) δ ppm 8.21 (t, J = 1.51 Hz, 1H), 7.96 (td, J = 1.44, 7.83 Hz, 1H), 7.84 (ddd, J = 1.24, 1.92, 7.83 Hz, 1H), 7.49−7.61 (m, 1H), 7.30 (d, J = 8.24 Hz, 1H), 7.24 (d, J = 1.92 Hz, 1H), 7.13−7.21 (m, 1H), 5.47 (d, J = 1.92 Hz, 1H), 4.11 (dd, J = 1.79, 3.43 Hz, 1H), 3.94 (s, 3H), 3.92 (s, 3H), 3.86−4.03 (m, 1H), 3.67−3.86 (m, 4H). MS (ESI): found $[M + Na]^+$, 443.1.

3′-Chloro-4′-(α-D-mannopyranosyloxy)-*N*-methylbiphenyl-3-carboxamide (5a). **5a** was prepared using the same procedure as for **5b**. Yield: 59%. ^{1}H NMR (300 MHz, methanol-d_4) δ ppm 8.03 (t, J = 1.51 Hz, 1H), 7.69−7.83 (m, 3H), 7.32−7.67 (m, 3H), 5.60 (d, J = 1.65 Hz, 1H), 4.12 (dd, J = 1.79, 3.43 Hz, 1H), 4.01 (dd, J = 3.57, 9.34 Hz, 1H), 3.69−3.84 (m, 3H), 3.61−3.69 (m, 1H), 2.95 (s, 3H). MS (ESI): found $[M + Na]^+$, 424.1.

4′-(α-D-Mannopyranosyloxy)-*N*-methyl-3′-(trifluoromethyl)-biphenyl-3-carboxamide (5c). **5c** was prepared using the same procedure as for **5b**. Yield: 65%. ^{1}H NMR (300 MHz, methanol-d_4) δ ppm 7.98 (t, J = 1.65 Hz, 1H), 7.77−7.87 (m, 2H), 7.65−7.77 (m, 2H), 7.42−7.60 (m, 2H), 5.58 (d, J = 1.65 Hz, 1H), 3.99 (dd, J = 1.79, 3.43 Hz, 1H), 3.81−3.91 (m, 1H), 3.59−3.80 (m, 3H), 3.45−3.58 (m, 1H), 2.87 (s, 3H). MS (ESI): found $[M + H]^+$, 458.1.

Dimethyl 4-(α-D-Mannopyranosyloxy)biphenyl-2,3′-dicarboxylate (6). Methyl 5-Hydroxy-2-(3-methoxycarbonylphenyl)benzoate. The reactants of methyl 2-bromo-5-hydroxybenzoate (0.231 g, 1 mmol), 3-methoxycarbonylphenylboronic acid (0.214 g, 1.2 mmol), palladium acetate (0.022 g, 0.1 mmol), potassium carbonate (0.346 g, 2.5 mmol), and tetrabutylammonium bromide (0.322 g, 1 mmol) in 1.2 mL of water were heated with stirring at 70 °C for 1 h and 20 min in a sealed vial by microwave. Then the mixture was partitioned between AcOEt and 1 N HCl aqueous solution. The organic layer was collected, dried with Na_2SO_4, then concentrated. The resulting residue was purified by silica gel chromatography with AcOEt/Hex combinations as eluent, giving the title compound (0.240 g) in 84% yield. ^{1}H NMR (300 MHz, DMSO-d_6) δ ppm 10.02 (s, 1H), 7.90 (td, J = 2.03, 6.66 Hz, 1H), 7.72−7.81 (m, 1H), 7.45−7.60 (m, 2H), 7.28 (d, J = 8.52 Hz, 1H), 7.16 (d, J = 2.47 Hz, 1H), 7.03 (dd, J = 2.61, 8.38 Hz, 1H), 3.86 (s, 3H), 3.56 (s, 3H). MS (ESI): found $[M + Na]^+$, 309.2.

Dimethyl 4-(α-D-Mannopyranosyloxy)biphenyl-2,3′-dicarboxylate (6). **6** was prepared via glycosidation between α-D-mannose pentaacetate and methyl 5-hydroxy-2-(3-methoxycarbonylphenyl)-benzoate following the procedure previously described.[25] Yield: 73%. ^{1}H NMR (300 MHz, methanol-d_4) δ ppm 3.56−3.68 (m, 4 H), 3.68−3.84 (m, 3 H), 3.86−3.98 (m, 4 H), 4.06 (dd, J = 3.30, 1.92 Hz, 1 H), 5.60 (d, J = 1.92 Hz, 1 H), 7.29−7.43 (m, 2 H), 7.45−7.53 (m, 2 H), 7.56 (d, J = 2.47 Hz, 1 H), 7.84−7.92 (m, 1 H), 7.93−8.04 (m, 1 H). MS (ESI): found $[M + H]^+$, 449.0.

4′-(α-D-Mannopyranosyloxy)-*N*,*N*′-dimethyl-3′-(trifluoromethyl)biphenyl-3,5-dicarboxamide (7) and *N*1,*N*3-Dimethyl-5-(4,4,5,5-tetramethyl-1,3,2-dioxaborolan-2-yl)benzene-1,3-dicarboxamide (9). Dimethyl 5-bromobenzene-1,3-dicarboxylate (10.6 g, 36.8 mmol) was dissolved in a 33 wt % solution of methylamine in EtOH (30 mL), and the mixture was stirred for 6 h at room temperature. The precipitate that formed during the reaction was filtered to give 5.3 g (53%) of the intermediate 5-bromo-*N*1,*N*3-dimethylbenzene-1,3-dicarboxamide as a white solid. Concentration of the remaining filtrate yielded an additional 4.6 g (46%) of product. 5-Bromo-*N*1,*N*3-dimethylbenzene-1,3-dicarboxamide (5.3 g, 19.5 mmol), Pd(dppf)Cl_2 (0.87 g, 1.2 mmol), bis(pinacolato)diboron (6.1 g, 24 mmol), and potassium acetate (7.8 g, 80 mmol) were dissolved in DMSO (100 mL). The solution was stirred under vacuum and then repressurized with nitrogen. This process was repeated 3 times, and then the resultant mixture was stirred at 80 °C for 5 h under a nitrogen atmosphere. After removal of the solvent under high vacuum, the crude material was purified by silica gel chromatography to give **9** as a light tan solid (2.2 g, 35%). ^{1}H NMR (300 MHz, DMSO-d_6) δ ppm 8.63 (m, 2H), 8.41 (t, J = 1.51 Hz, 1H), 8.23 (d, J = 1.65 Hz, 2H), 2.79 (d, J = 4.40 Hz, 6H), 1.33 (s, 12H). MS (ESI): found $[M + H]^+$, 319.2.

4′-(α-D-Mannopyranosyloxy)-*N*,*N*′-dimethyl-3′-(trifluoromethyl)biphenyl-3,5-dicarboxamide (7). With the procedure outlined in the synthesis of **5b** with 4-bromo-2-(trifluoromethyl)phenyl 2,3,4,6-tetra-*O*-acetyl-α-D-mannopyranoside (0.57 g) and **9** (0.48 g), the title compound (0.340 g) was obtained in 69% yield for the two steps. ^{1}H NMR (300 MHz, methanol-d_4) δ ppm 8.17−8.24 (m, 1H), 8.14 (d, J = 1.65 Hz, 2H), 7.92 (d, J = 1.92 Hz, 1H), 7.87 (dd, J = 2.20, 8.79 Hz, 1H), 7.57 (d, J = 8.79 Hz, 1H), 5.64 (d, J = 1.65 Hz, 1H), 4.04 (dd, J = 1.65, 3.30 Hz, 1H), 3.87−3.96 (dd, 1H), 3.64−3.83 (m, 3H), 3.48−3.63 (m, 1H), 2.93 (s, 6H). MS (ESI): found $[M + H]^+$, 515.1.

4′-(α-D-Mannopyranosyloxy)-*N*,*N*′,3′-trimethylbiphenyl-3,5-dicarboxamide (8). **8** was prepared using the same procedure as for **5b** with **9** as the Suzuki coupling partner. Yield: 56%. ^{1}H NMR (300 MHz, methanol-d_4) δ ppm 8.09−8.23 (m, 3H), 7.46−7.59 (m, 2H), 7.33 (d, J = 8.52 Hz, 1H), 5.57 (d, J = 1.92 Hz, 1H), 4.08 (dd, J = 1.92, 3.30 Hz, 1H), 3.97 (dd, J = 3.43, 9.48 Hz, 1H), 3.67−3.85 (m, 3H), 3.60 (ddd, J = 2.47, 5.01, 7.35 Hz, 1H), 2.96 (s, 6H), 2.32 (s, 3H). MS (ESI): found $[M + H]^+$, 461.2.

Procedure for the Preparation of Mannosides via Amide Coupling Reaction: *N*-(2-Hydroxyethyl)-4′-(α-D-mannopyranosyloxy)biphenyl-3-carboxamide (10a). Under nitrogen atmosphere at 0 °C anhydrous DMF (5 mL) was added into a round-bottom flask containing 4′-(α-D-mannopyranosyloxy)biphenyl-3-carboxylic acid[25] (0.038 g, 0.1 mmol) and HATU (0.046 g, 0.12 mmol). After the mixture was stirred for 10 min, aminoethanol (0.007 g, 0.12 mmol) and then *N*,*N*-diisopropylethylamine (0.039 g, 0.3 mmol) were added. The mixture was stirred overnight while being warmed to room temperature naturally. The solvent was removed, and the residue was purified by HPLC (C18, 15 mm × 150 mm column; eluent, acetonitrile/water (0.1% TFA)) to give the title compound (0.032 g) in 76% yield. ^{1}H NMR (300 MHz,

deuterium oxide) δ ppm 3.53−3.63 (m, 2 H), 3.68−3.94 (m, 6 H), 4.11 (dd, J = 9.20, 3.43 Hz, 1 H), 4.22 (dd, J = 3.30, 1.92 Hz, 1 H), 5.66 (d, J = 1.65 Hz, 1 H), 7.21 (d, J = 8.79 Hz, 2 H), 7.47−7.62 (m, 3 H), 7.66−7.78 (m, 2 H), 7.87 (t, J = 1.65 Hz, 1 H). MS (ESI): found $[M + H]^+$, 420.1.

N-(2-Aminoethyl)-4′-(α-D-mannopyranosyloxy)biphenyl-3-carboxamide (10b). **10b** was prepared using the same procedure as for **10a**. Yield: 60%. ^{1}H NMR (300 MHz, methanol-d_4) δ ppm 3.14−3.26 (m, 2 H), 3.57−3.66 (m, 1 H), 3.66−3.83 (m, 5 H), 3.87−4.00 (m, 1 H), 4.03 (dd, J = 3.30, 1.92 Hz, 1 H), 5.49−5.62 (m, 1 H), 7.19−7.31 (m, 2 H), 7.49−7.59 (m, 1 H), 7.59−7.72 (m, 2 H), 7.75−7.89 (m, 2 H), 8.03−8.21 (m, 1 H). MS (ESI): found $[M + H]^+$, 419.2.

3′-(Piperazin-1-ylcarbonyl)biphenyl-4-yl α-D-mannopyranoside (10c). **10c** was prepared using the same procedure as for **10a**. Yield: 65%. ^{1}H NMR (300 MHz, methanol-d_4) δ ppm 3.54−3.67 (m, 1 H), 3.67−3.85 (m, 4 H), 3.85−3.99 (m, 4 H), 4.03 (dd, J = 3.30, 1.92 Hz, 1 H), 5.54 (d, J = 1.65 Hz, 1 H), 7.19−7.29 (m, 2 H), 7.42 (dt, J = 7.69, 1.24 Hz, 1 H), 7.50−7.64 (m, 3 H), 7.67−7.79 (m, 2 H). MS (ESI): found $[M + H]^+$, 445.3.

3′-[(4-Methylpiperazin-1-yl)carbonyl]biphenyl-4-yl α-D-mannopyranoside (10d). **10d** was prepared using the same procedure as for **10a**. Yield: 87%. ^{1}H NMR (300 MHz, methanol-d_4) δ ppm 2.96 (s, 3 H), 3.05−3.65 (m, 9 H), 3.68−3.85 (m, 3 H), 3.87−3.97 (m, 1 H), 4.03 (dd, J = 3.30, 1.92 Hz, 1 H), 5.54 (d, J = 1.65 Hz, 1 H), 7.17−7.30 (m, 2 H), 7.42 (dt, J = 7.62, 1.27 Hz, 1 H), 7.50−7.66 (m, 3 H), 7.67−7.80 (m, 2 H). MS (ESI): found $[M + H]^+$, 459.0.

4′-(α-D-Mannopyranosyloxy)-N-(pyridin-4-yl)biphenyl-3-carboxamide (10e). **10e** was prepared using the same procedure as for **10a**. Yield: 93%. ^{1}H NMR (300 MHz, methanol-d_4) δ ppm 3.57−3.69 (m, 1 H), 3.69−3.84 (m, 3 H), 3.93 (dd, J = 9.34, 3.30 Hz, 1 H), 4.04 (dd, J = 3.30, 1.92 Hz, 1 H), 5.56 (d, J = 1.65 Hz, 1 H), 7.18−7.37 (m, 2 H), 7.57−7.78 (m, 3 H), 7.82−8.06 (m, 2 H), 8.24 (t, J = 1.65 Hz, 1 H), 8.36−8.51 (m, 2 H), 8.68 (d, J = 7.42 Hz, 2 H). MS (ESI): found $[M + H]^+$, 453.1.

4′-(α-D-Mannopyranosyloxy)-N-(pyridin-3-yl)biphenyl-3-carboxamide (10f). **10f** was prepared using the same procedure as for **10a**. Yield: 75%. ^{1}H NMR (300 MHz, methanol-d_4) δ ppm 3.55−3.68 (m, 1 H), 3.68−3.85 (m, 3 H), 3.88−3.98 (m, 1 H), 4.04 (dd, J = 3.43, 1.79 Hz, 1 H), 5.56 (d, J = 1.92 Hz, 1 H), 7.20−7.32 (m, 2 H), 7.52−7.73 (m, 3 H), 7.80−7.91 (m, 1 H), 7.91−7.99 (m, 1 H), 8.04 (dd, J = 8.65, 5.63 Hz, 1 H), 8.23 (t, J = 1.65 Hz, 1 H), 8.59 (d, J = 5.49 Hz, 1 H), 8.67−8.79 (m, 1 H), 9.55 (s, 1 H). MS (ESI): found $[M + H]^+$, 453.2.

Procedure for the Preparation of Biphenyl Mannoside Derivatives through Suzuki Coupling Reaction with 4-(4,4,5,5-Tetramethyl-1,3,2-dioxaborolan-2-yl)phenyl 2,3,4,6-Tetra-O-acetyl-α-D-mannopyranoside (11) as Intermediates: Methyl 5-[4-(α-D-Mannopyranosyloxy)phenyl]pyridine-3-carboxylate (12b). **4-(4,4,5,5-Tetramethyl-1,3,2-dioxaborolan-2-yl)phenyl 2,3,4,6-Tetra-O-acetyl-α-D-mannopyranoside (11).** Under nitrogen atmosphere, a mixture of 4-bromophenyl 2,3,4,6-tetra-*O*-acetyl-α-D-mannopyranoside (2.791 g, 5.55 mmol), bis(pinacolato)diboron (1.690 g, 6.66 mmol), potassium acetate (2.177 g, 22.18 mmol), and (1.1′-bis(diphenylphosohino)ferrocene)dichloropalladium(II) (0.244 g, 0.33 mmol) in DMSO (50 mL) was heated at 80 °C with stirring for 2.5 h. The solvent was removed and the resulting residue was purified by silica gel chromatography with hexane/ethyl acetate combinations as eluent to give **11** (2.48 g) in 81% yield. ^{1}H NMR (300 MHz, chloroform-*d*) δ ppm 1.33 (s, 12 H), 1.98−2.12 (m, 9 H), 2.20 (s, 3 H), 3.93−4.19 (m, 2 H), 4.21−4.36 (m, 1 H), 5.32−5.42 (m, 1 H), 5.45 (dd, J = 3.57, 1.92 Hz, 1 H), 5.51−5.62 (m, 2 H), 7.00−7.15 (m, 2 H), 7.67−7.84 (m, 2 H). MS (ESI): found $[M + Na]^+$, 573.2.

Methyl 5-[4-(α-D-Mannopyranosyloxy)phenyl]pyridine-3-carboxylate (12b). Under nitrogen atmosphere, a mixture of **11** (0.132 g, 0.24 mmol), methyl 5-bromonicotinate (0.043 g, 0.2 mmol), cesium carbonate (0.196 g, 0.6 mmol), and tetrakis(triphenylphosphine)palladium (0.023 g, 0.02 mmol) in dioxane/water (5 mL/1 mL) was heated at 80 °C with stirring for 1 h. After cooling, the mixture was filtered through a silica gel column to remove the metal catalyst and salts with hexane/ethyl acetate (2/1) containing 2% triethylamine as eluent. The filtrate was concentrated, then dried in vacuo. Into the residue, 6 mL of methanol with a catalytic amount of sodium methoxide (0.02 M) was added, and the mixture was stirred at room temperature overnight. The solvent was removed. The resulting residue was purified by silica gel chromatography with CH_2Cl_2/MeOH combinations containing 2% NH_3/H_2O as eluent, giving rise to **12b** (0.031 g) in 40% yield. ^{1}H NMR (300 MHz, CD_3OD) δ ppm 3.53−3.65 (m, 1 H), 3.67−3.83 (m, 3 H), 3.89−3.96 (m, 1 H), 3.99 (s, 3 H), 4.04 (dd, J = 3.43, 1.79 Hz, 1 H), 5.57 (d, J = 1.92 Hz, 1 H), 7.22−7.37 (m, 2 H), 7.58−7.73 (m, 2 H), 8.54 (t, J = 2.06 Hz, 1 H), 8.97 (d, J = 2.20 Hz, 1 H), 9.04 (d, J = 1.92 Hz, 1 H). MS (ESI): found $[M + H]^+$, 392.1.

Methyl 4-[4-(α-D-Mannopyranosyloxy)phenyl]pyridine-2-carboxylate (12a). **12a** was prepared using the same procedure as for **12b** and was purified by HPLC (C18, 15 mm × 150 mm column; eluent, acetonitrile/water (0.1% TFA)). Yield: 15%. ^{1}H NMR (300 MHz, methanol-d_4) δ ppm 3.51−3.63 (m, 1 H), 3.65−3.84 (m, 3 H), 3.88−3.95 (m, 1 H), 4.00−4.13 (m, 4 H), 5.62 (d, J = 1.65 Hz, 1 H), 7.28−7.40 (m, 2 H), 7.82−7.95 (m, 2 H), 8.13 (dd, J = 5.49, 1.92 Hz, 1 H), 8.55 (d, J = 1.65 Hz, 1 H), 8.73 (d, J = 5.49 Hz, 1 H). MS (ESI): found $[M + H]^+$, 392.2.

Methyl 3-(Carbamoylamino)-5-[4-(α-D-mannopyranosyloxy)-phenyl]thiophene-2-carboxylate (13a). **13a** was prepared using the same procedure as for **12b** and was purified by HPLC (C18, 15 mm × 150 mm column; eluent, acetonitrile/water (0.1% TFA)). Yield: 10%. ^{1}H NMR (300 MHz, methanol-d_4) δ ppm 3.58 (ddd, J = 7.21, 4.88, 2.47 Hz, 1 H), 3.66−3.83 (m, 3 H), 3.83−3.96 (m, 4 H), 4.02 (dd, J = 3.30, 1.92 Hz, 1 H), 5.54 (d, J = 1.65 Hz, 1 H), 7.12−7.27 (m, 2 H), 7.56−7.69 (m, 2 H), 8.12 (s, 1 H). MS (ESI): found $[M + H]^+$, 455.1.

Methyl 5-[4-(α-D-Mannopyranosyloxy)phenyl]thiophene-2-carboxylate (13b). **13b** was prepared using the same procedure as for **12b** and was purified by silica gel chromatography with CH_2Cl_2/MeOH combinations. Yield: 23%. ^{1}H NMR (300 MHz, methanol-d_4) δ ppm 3.53−3.62 (m, 1 H), 3.68−3.81 (m, 3 H), 3.85−3.94 (m, 4 H), 4.02 (dd, J = 3.60, 2.1 Hz, 1 H), 5.54 (d, J = 1.8 Hz, 1 H), 7.19 (m, 2 H), 7.34 (d, J = 3.9 Hz, 1 H), 7.64 (m, 2 H), 7.75 (d, J = 3.9 Hz, 1 H). MS (ESI): found $[M + Na]^+$, 419.1.

(5-Bromo-3-thienyl)urea (16). Under nitrogen atmosphere *N,N*-diisopropylethylamine (0.390 g, 3 mmol) was added to a solution of 5-bromothiophene-3-carboxylic acid (0.207 g, 1 mmol) and DPPA (0.330 g, 1.2 mmol) in dioxane (5 mL) at room temperature. After being stirred for 30 min, the mixture was heated at 85 °C for 1.5 h. After the mixture cooled to room temperature, 0.5 M ammonia solution in dioxane (12 mL) was added. After 30 min, the solvents were removed and the resulting residue was purified by silica gel chromatography with CH_2Cl_2/MeOH combinations to give (5-bromo-3-thienyl)urea (0.072 g) in 32% yield. ^{1}H NMR (300 MHz, DMSO-d_6) δ ppm 8.80 (s, 1H), 7.09 (s, 2H), 5.87 (s, 2H). MS (ESI): found $[M + H]^+$, 223.0.

1-{5-[4-(α-D-Mannopyranosyloxy)phenyl]thiophen-3-yl}urea (13c). **13c** was prepared using the same procedure as for **12b** and was purified by HPLC (C18, 15 mm × 150 mm column; eluent, acetonitrile/water (0.1% TFA)). Yield: 80%. ^{1}H NMR (300 MHz, methanol-d_4/acetonitrile-d_3(3/1)) δ 7.50−7.62 (m, 2H), 7.11−7.21 (m, 3H), 7.08 (d, J = 1.37 Hz, 1H), 5.53 (d, J = 1.65 Hz, 1H), 4.02 (dd, J = 1.92, 3.30 Hz, 1H), 3.82−3.95 (m, 1H), 3.66−3.81 (m, 3H), 3.51−3.64 (m, 1H). MS (ESI): found $[M + H]^+$, 397.1.

Methyl 5-[4-(α-D-Mannopyranosyloxy)phenyl]thiophene-3-carboxylate (13d). **13d** was prepared using the same procedure as for **12b** and was purified by silica gel chromatography with CH_2Cl_2/MeOH combinations. Yield: 33%. ^{1}H NMR (300 MHz, methanol-d_4) δ ppm 3.55−3.63 (m, 1 H), 3.68−3.81 (m, 3 H), 3.84−3.94 (m, 4 H), 4.02 (dd, J = 3.30, 1.8 Hz, 1 H), 5.53 (d, J = 1.8 Hz, 1 H), 7.18 (m, 2 H), 7.59 (m, 2 H), 7.64 (d, J = 1.5 Hz, 1 H), 8.11 (d, J = 1.5 Hz, 1 H). MS (ESI): found $[M + Na]^+$, 419.1.

4-(Isoquinolin-7-yl)phenyl α-D-Mannopyranoside (14a). **14a** was prepared using the same procedure as for **12b** and was purified by HPLC (C18, 15 mm × 150 mm column; eluent, acetonitrile/water (0.1% TFA)). Yield: 73%. ^{1}H NMR (300 MHz, methanol-d_4) δ 9.73 (s, 1H), 8.59−8.71 (m, 1H), 8.47−8.58 (m, 2H), 8.42 (d, J = 6.59 Hz, 1H),

dx.doi.org/10.1021/jm300165m | J. Med. Chem. 2012, 55, 3945−3959

8.33 (d, J = 8.79 Hz, 1H), 7.76−7.89 (m, 2H), 7.25−7.41 (m, 2H), 5.60 (d, J = 1.92 Hz, 1H), 4.06 (dd, J = 1.92, 3.30 Hz, 1H), 3.87−4.00 (m, 1H), 3.68−3.87 (m, 3H), 3.55−3.68 (m, 1H). MS (ESI): found $[M + H]^+$, 384.2.

4-(Quinazolin-6-yl)phenyl α-D-Mannopyranoside (14b). **14b** was prepared using the same procedure as for **12b.** Yield: 28%. ^{1}H NMR (300 MHz, methanol-d_4) δ 9.51 (s, 1H), 9.15 (s, 1H), 8.21−8.35 (m, 2H), 8.02 (d, J = 8.52 Hz, 1H), 7.63−7.80 (m, J = 8.79 Hz, 2H), 7.14−7.32 (m, J = 8.79 Hz, 2H), 5.50 (d, J = 1.37 Hz, 1H), 3.94−4.03 (m, 1H), 3.80−3.94 (m, 1H), 3.62−3.80 (m, 3H), 3.48−3.62 (m, 1H). MS (ESI): found $[M + H]^+$, 385.1.

4-(Isoquinolin-5-yl)phenyl α-D-Mannopyranoside (15a). **15a** was prepared using the same procedure as for **12b** and was purified by HPLC (C18, 15 mm × 150 mm column; eluent, acetonitrile/water (0.1% TFA)). Yield: 90%. ^{1}H NMR (300 MHz, methanol-d_4) δ 9.80 (s, 1H), 8.45−8.60 (m, 2H), 8.35 (d, J = 6.59 Hz, 1H), 8.01−8.21 (m, 2H), 7.45−7.55 (m, 2H), 7.31−7.42 (m, 2H), 5.62 (d, J = 1.92 Hz, 1H), 4.07 (dd, J = 1.92, 3.30 Hz, 1H), 3.89−3.99 (m, 1H), 3.70−3.86 (m, 3H), 3.60−3.69 (m, 1H). MS (ESI): found $[M + H]^+$, 384.2.

4-(1-Oxo-1,2-dihydroisoquinolin-7-yl)phenyl α-D-Mannopyranoside (15b). **15b** was prepared using the same procedure as for **12b** and was purified by HPLC (C18, 15 mm × 150 mm column; eluent, acetonitrile/water (0.1% TFA)). Yield: 75%. ^{1}H NMR (300 MHz, methanol-d_4) δ 8.51 (d, J = 2.20 Hz, 1H), 7.93−8.05 (m, 1H), 7.62−7.77 (m, 3H), 7.21−7.31 (m, 2H), 7.18 (d, J = 7.14 Hz, 1H), 6.71 (d, J = 7.14 Hz, 1H), 5.56 (d, J = 1.92 Hz, 1H), 4.04 (dd, J = 1.92, 3.57 Hz, 1H), 3.88−4.00 (m, 1H), 3.69−3.87 (m, 3H), 3.57−3.69 (m, 1H). MS (ESI): found $[M + H]^+$, 400.2.

Affinity Measurement by Biolayer Interferometry. Samples or buffer (200 μL per well) was dispensed into 96-well microtiter plates (Greiner Bio-One, Monroe, NC) and maintained at 30 °C with 1000 rpm shaking. Premanufactured pins for individual assays were made by biotinylating FimH lectin domain[25] at a 1:1 molar ratio with NHS-PEO4-biotin (Thermo Fisher, Rockford, IL), diluting it to 50 μg/mL in 20 mM HEPES, pH 7.5, 150 mM NaCl (HBS), immobilizing it on high-binding streptavidin-coated biosensor tips (Super Streptavidin, FortéBio, Inc., Menlo Park, CA) for 10 min at 30 °C, blocking the pins with 10 μg/mL biocytin for 2 min, washing in HBS for 1 h, and rinsing in 15% sucrose in HBS. Pins were then air-dried for 30 min and stored in their original packaging with a desiccant packet. Assays were performed by rewetting premade pins with HBS for 15 min, then storing them in fresh HBS until use. Individual affinity assays were performed on an Octet Red instrument (FortéBio, Inc., Menlo Park, CA) and consisted of a short baseline measurement followed by incubation of pins for 10 min with seven 2-fold dilutions (in HBS) of compound in a concentration range experimentally determined to give well-measured association and dissociation kinetics, then a 30 min dissociation phase in HBS. Each experimental pin was referenced to a biocytin-blocked pin to control for instrument drift and a second biocytin-blocked pin that was passed through a duplicate experiment in the same 96-well plate to control for nonspecific binding of the compound to the pin. Kinetics data and affinity constants were generated automatically by the global fitting protocol in ForteBio Data Analysis, version 6.3. Typical signal for compound binding was approximately 0.2 "nm shift" units, while the noise level of the instrument is around 0.0025 nm.

DSF Method. FimH lectin domain (residues 1−158 of UPEC J96 FimH, without an affinity tag)[22] was purified as described previously. An amount of 5 μg of FimH in 5 μL of HBS was mixed with HBS to yield a final volume of 50 μL containing compound at a final concentration of 100 μM and a "5×" final concentration of SYPRO Orange (sold as a "5000×" stock in DMSO and mixed with HBS to a working stock of 50× immediately before use, Life Technologies Inc.; Grand Island, NY) . Compounds were diluted to 100 μM from stocks in DMSO and compared to matched control wells with FimH alone plus 0.2% DMSO. Then 50 μL mixtures were placed in 96-well clear-bottom PCR plates and subjected to a melt curve from 20 to 90 °C in 0.5 °C increments of 15 s each followed by a fluorescence read of the "HEX" channel in a Bio-Rad CFX96 thermocycler (Bio-Rad, Hercules, CA). Melt curves were fitted to the Boltzmann equation to determine the melting temperature (T_m) ($y = A_2 + (A_1 - A_2)/(1 + \exp((x - x_0)/dx))$ where x_0 is the T_m) using OriginPro 8 (OriginLab, Northampton MA). Melting temperatures are represented as the mean of three replicates plus or minus 1 standard deviation in Figure 4.

PK Studies. Compound levels in mouse urine and plasma were made using an AB Sciex API-4000 QTrap (AB Sciex, Foster City, CA) as previously described.[36] Selected reaction monitoring (SRM) mode quantification was performed using the following MS/MS transitions [precursor mass/charge ratio (m/z)/product m/z]: compound **3**, 447/285; compound **5a**, 424/262; compound **5b**, 404/242; compound **5c**, 548/296; compound **7**, 515/353; compound **8**, 461/299; compound **3** R group, 285/254.

PAMPA Method. Materials. The assay was carried out using Multiscreen PVDF 96-well plates (Millipore, Billerica, MA) using the company's transporter receiver plate. The lipid (dioleyoylphosphotidylcholine (DOPC)/stearic acid (80:20, wt %) in dodecane was obtained from avanti polar lipids (Alabaster, AL). Hank's buffered salt solution (HBSS), pH 7.4, was obtained from MediaTech (Manassas, VA).

Methods. Each of the test compounds was diluted to 2.5 mM in DMSO (Sigma, St. Louis, MO) and further diluted prior to testing to 2.5 μM in HBSS, pH 7.4. The assay was performed using a Millipore 96-well multiscreen-IP PAMPA plate, and 5 μL of the lipid suspension was directly added to the PVDF membrane of the filter plate. Immediately following the addition of the lipid to the membrane, 200 μL of HBSS solution containing the test compound was added to the donor (upper) chamber. HBSS (300 μL) was also added to the receiver plate, and the filter and receiver plates were assembled and incubated overnight at room temperature in a moistened sealed bag to prevent evaporation. The concentration in the receiver plate as well as an equilibrium plate, which represents a theoretical, partition-free sample, was determined by HPLC−tandem mass spectrometry. Analysis of each compound was performed in triplicate.

Analysis. Analyses of both the acceptor and equilibrium samples were performed using an AB 3200 triple quadrupole mass spectrometer linked to a Shimadzu DGU-20A HPLC instrument with a Prevail C18 column (3 μm, 2.1 mm × 10 mm) with a flow rate of 0.35 mL/min. The mobile phase used was A (0.1% formic acid in water) and B (0.1% formic acid in methanol). The elution gradient method is shown in the Table 5. Data acquisition and peak height determination were performed using Analyst, version 1.4.2.

Table 5

time, min	solvent A, %	solvent B, %
0.01	95	5
0.50	95	5
1.00	5	95
2.00	5	95
2.01	95	5
6.01	stop	

Calculations. The $\log_{10}$ of the effective permeability ($\log P_e$) was calculated using the following equation

$$\log P_e = \log\left\{C \times -\ln\left(1 - \frac{[\text{drug}]_{\text{acceptor}}}{[\text{drug}]_{\text{equilibrium}}}\right)\right\}$$

where

$$C = \frac{V_D V_A}{(V_D + V_A)(\text{area})(\text{time})}$$

where the drug concentration is the peak areas for the analyte and V_D and V_A are the volume of the donor and acceptor compartments, respectively. The area is the surface area of the PVDF membrane

(0.11 cm^2), and time is the incubation in seconds (64 800 s). Each value is the mean of triplicates performed on the same day.

■ ASSOCIATED CONTENT

Supporting Information

NMR spectra of compounds. This material is available free of charge via the Internet at http://pubs.acs.org.

■ AUTHOR INFORMATION

Corresponding Author

*For S.J.H.: phone, 314-362-7059; e-mail, hultgren@borcim.wustl.edu. For J.W.J.: phone, 314-362-0509; e-mail, janetkaj@biochem.wustl.edu.

Notes

The authors declare no competing financial interest.

■ ACKNOWLEDGMENTS

This work was completed in part by funding from the National Institutes of Health (NIH) American Recovery and Reinvestment Act (ARRA) Challenge Grant 1RC1DK086378 and a Washington University OTM Bear Cub Grant.

■ ABBREVIATIONS USED

UTI, urinary tract infection; UPEC, uropathogenic *E. coli*; PAMPA, parallel artificial membrane permeability assay; IBC, intracellular bacterial community; HAI, hemagglutination inhibition; SAR, structure−activity relationship; PK, pharmacokinetic; PSA, polar surface area; DSF, differential scanning fluorimetry; IC_{50}, half maximal inhibitory concentration; $EC_{>90}$, over 90% of maximal effective concentration; po, oral; HATU, 2-(7-aza-1*H*-benzotriazole-1-yl)-1,1,3,3-tetramethyluronium hexafluorophosphate; DPPA, diphenylphosphorylazide; methyl man., methyl α-D-mannoside; butyl man., butyl α-D-mannoside; phenyl αD man., phenyl α-D-mannoside

■ REFERENCES

(1) (a) Waksman, G.; Hultgren, S. J. Structural biology of the chaperoneusher pathway of pilus biogenesis. *Nat. Rev. Microbiol.* **2009**, *7*, 765−774. (b) Mulvey, M. A. Adhesion and entry of uropathogenic *Escherichia coli*. *Cell. Microbiol.* **2002**, *4*, 257−271. (c) Capitani, G.; Eidam, O.; Glockshuber, R.; Grutter, M. G. Structural and functional insights into the assembly of type 1 pili from *Escherichia coli*. *Microbes Infect.* **2006**, *8*, 2284−2290. (d) Bouckaert, J.; Mackenzie, J.; De Paz, J. L.; Chipwaza, B.; Choudhury, D.; Zavialov, A.; Mannerstedt, K.; Anderson, J.; Piérard, D.; Wyns, L.; Seeberger, P. H.; Oscarson, S.; De Greve, H.; Knight, S. D. The affinity of the FimH fimbrial adhesin is receptor-driven and quasi-independent of *Escherichia coli* pathotypes. *Mol. Microbiol.* **2006**, *61*, 1556−1568.

(2) (a) Yu, J.; Lin, J. H.; Wu, X. R.; Sun, T. T. Uroplakins Ia and Ib, two major differentiation products of bladder epithelium, belong to a family of four transmembrane domain (4TM) proteins. *J. Cell Biol.* **1994**, *125*, 171−182. (b) Sun, T. T.; Zhao, H.; Provet, J.; Aebi, U.; Wu, X. R. Formation of asymmetric unit membrane during urothelial differentiation. *Mol. Biol. Rep.* **1996**, *23*, 3−11.

(3) Martinez, J. J.; Mulvey, M. A.; Schilling, J. D.; Pinkner, J. S.; Hultgren, S. J. Type 1 pilus-mediated bacterial invasion of bladder epithelial cells. *EMBO J.* **2000**, *19*, 2803−2812.

(4) Malaviya, R.; Ross, E.; MacGregor, J. I.; Ikeda, T.; Little, J. R.; Jakschik, B. A.; Abraham, S. N. Mast cell phagocytosis of FimH-expressing enterobacteria. *J. Immunol.* **1994**, *152*, 1907−1914.

(5) Mulvey, M. A.; Lopez-Boado, Y. S.; Wilson, C. L.; Roth, R.; Parks, W. C.; Heuser, J.; Hultgren, S. J. Induction and evasion of host defenses by type 1-piliated uropathogenic *Escherichia coli*. *Science* **1998**, *282*, 1494−1497.

(6) Bishop, B. L.; Duncan, M. J.; Song, J.; Li, G.; Zaas, D.; Abraham, S. N. Cyclic AMP-regulated exocytosis of *Escherichia coli* from infected bladder epithelial cells. *Nat. Med.* **2007**, *13*, 625−630.

(7) Eto, D. S.; Jones, T. A.; Sundsbak, J. L.; Mulvey, M. A. Integrin-mediated host cell invasion by type 1-piliated uropathogenic *Escherichia coli*. *PLoS Pathog.* **2007**, *3*, e100.

(8) (a) Chen, S. L.; Hung, C. S.; Pinkner, J. S.; Walker, J. N.; Cusumano, C. K.; Li, Z.; Bouckaert, J.; Gordon, J. I.; Hultgren, S. J. Positive selection identifies an in vivo role for FimH during urinary tract infection in addition to mannose binding. *Proc. Natl. Acad. Sci. U.S.A.* **2009**, *106*, 22439−22444. (b) Justice, S. S.; Hung, C.; Theriot, J. A.; Fletcher, D. A.; Anderson, G. G.; Footer, M. J.; Hultgren, S. J. Differentiation and developmental pathways of uropathogenic *Escherichia coli* in urinary tract pathogenesis. *Proc. Natl. Acad. Sci. U.S.A.* **2004**, *101*, 1333−1338. (c) Wright, K. J.; Seed, P. C.; Hultgren, S. J. Development of intracellular bacterial communities of uropathogenic *Escherichia coli* depends on type 1 pili. *Cell. Microbiol.* **2007**, *9*, 2230−2241. (d) Nicholson, T. F.; Watts, K. M.; Hunstad, D. A. OmpA of uropathogenic *Escherichia coli* promotes postinvasion pathogenesis of cystitis. *Infect. Immun.* **2009**, *77*, 5245−5251. (e) Justice, S. S.; Lauer, S. R.; Hultgren, S. J.; Hunstad, D. A. Maturation of intracellular *Escherichia coli* communities requires SurA. *Infect. Immun.* **2006**, *74*, 4793−4800. (f) Anderson, G. G.; Goller, C. C.; Justice, S. S.; Hultgren, S. J.; Seed, P. C. Polysaccharide capsule and sialic acid-mediated regulation promote biofilm-like intracellular bacterial communities during cystitis. *Infect. Immun.* **2010**, *78*, 963−975.

(9) Song, J.; Bishop, B. L.; Li, G.; Grady, R.; Stapleton, A.; Abraham, S. N. TLR4-mediated expulsion of bacteria from infected bladder epithelial cells. *Proc. Natl. Acad. Sci. U.S.A.* **2009**, *106*, 14966−14971.

(10) Anderson, G. G.; Palermo, J. J.; Schilling, J. D.; Roth, R.; Heuser, J.; Hultgren, S. J. Intracellular bacterial biofilm-like pods in urinary tract infections. *Science* **2003**, *301*, 105−107.

(11) (a) Shilling, J. D.; Lorenz, R. G.; Hultgren, S. J. Effect of trimethoprim-sulfamethoxazole on recurrent bacteriuria and bacterial persistence in mice infected with uropathogenic *Escherichia coli*. *Infect. Immun.* **2002**, *70*, 7042−7049. (b) Mulvey, M. A.; Schilling, J. D.; Hultgren, S. J. Establishment of a persistent *Escherichia coli* reservoir during the acute phase of a bladder infection. *Infect. Immun.* **2001**, *69*, 452−459. (c) Mysorekar, I. U.; Hultgren, S. J. Mechanisms of uropathogenic *Escherichia coli* persistence and eradication from the urinary tract. *Proc. Natl. Acad. Sci. U.S.A.* **2006**, *103*, 14170−14175.

(12) Connell, H.; Agace, W.; Klemm, P.; Schembri, M.; Marild, S.; Svanborg, C. Type 1 fimbrial expression enhances *Escherichia coli* virulence for the urinary tract. *Proc. Natl. Acad. Sci. U.S.A.* **1996**, *93*, 9827−9832.

(13) Norinder, B. S.; Köves, B.; Yadav, M.; Brauner, A.; Svanborg, C. Do *Escherichia coli* strains causing acute cystitis have a distinct virulence repertoire? *Microb. Pathog.* **2012**, *52*, 10−16.

(14) Snyder, J. A.; Lloyd, A. L.; Lockatell, C. V.; Johnson, D. E.; Mobley, H. L. Role of phase variation of type 1 fimbriae in a uropathogenic *Escherichia coli* cystitis isolate during urinary tract infection. *Infect. Immun.* **2006**, *74*, 1387−1393.

(15) (a) Weissman, S. J.; Beskhlebnaya, V.; Chesnokova, V.; Chattopadhyay, S.; Stamm, W. E.; Hooton, T. M.; Sokurenko, E. V. Differential stability and trade-off effects of pathoadaptive mutations in the *Escherichia coli* FimH adhesin. *Infect. Immun.* **2007**, *75*, 3548−3555. (b) Ronald, L. S.; Yakovenko, O.; Yazvenko, N.; Chattopadhyay, S.; Aprikian, P.; Thomas, W. E.; Sokurenko, E. V. Adaptive mutations in the signal peptide of the type 1 fimbrial adhesin of uropathogenic *Escherichia coli*. *Proc. Natl. Acad. Sci. U.S.A.* **2008**, *105*, 10937−10942.

(16) Rosen, D. A.; Hooton, T. M.; Stamm, W. E.; Humphrey, P. A.; Hultgren, S. J. Detection of intracellular bacterial communities in human urinary tract infection. *PLoS Med.* **2007**, *4*, e329.

(17) (a) Langermann, S.; Palaszynski, S.; Barnhart, M.; Auguste, G.; Pinkner, J. S.; Burlein, J.; Barren, P.; Koenig, S.; Leath, S.; Jones, C. H.; Hultgren, S. J. Prevention of mucosal *Escherichia coli* infection by FimH-adhesin-based systemic vaccination. *Science* **1997**, *276*, 607−611. (b) Cegelski, L.; Pinkner, J. S.; Hammer, N. D.; Cusumano, C. K.;

Hung, C. S.; Chorell, E.; Aberg, V.; Walker, J. N.; Seed, P. C.; Almqvist, F.; Chapman, M. R.; Hultgren, S. J. Small-molecule inhibitors target *Escherichia coli* amyloid biogenesis and biofilm formation. *Nat. Chem. Biol.* **2009**, *5*, 913−919. (c) Pinkner, J. S.; Remaut, H.; Buelens, F.; Miller, E.; Åberg, V.; Pemberton, N.; Hedenström, M.; Larsson, A.; Seed, P.; Waksman, G.; Hultgren, S. J.; Almqvist, F. Rationally designed small compounds inhibit pilus biogenesis in uropathogenic bacteria. *Proc. Natl. Acad. Sci. U.S.A.* **2006**, *103*, 17897−17902.

(18) Review of small molecular FimH binding inhibitors: Hartmann, M.; Lindhorst, T. K. The bacterial lectin FimH, a target for drug discovery: carbohydrate inhibitors of type 1 fimbriae-mediated bacterial adhesion. *Eur. J. Org. Chem.* **2011**, 3583−3609.

(19) Firon, N.; Ashkenazi, S; Mirelman, D.; Ofek, I.; Sharon, N. Aromatic alpha-glycosides of mannose are powerful inhibitors of the adherence of type 1 fimbriated *Escherichia coli* to yeast and intestinal epithelial cells. *Infect. Immun.* **1987**, *55*, 472−476.

(20) (a) Almant, M.; Moreau, V.; Kovensky, J.; Bouckaert, J.; Gouin, S. G. Clustering of *Escherichia coli* type-1 fimbrial adhesins by using multimeric heptyl α-D-mannoside probes with a carbohydrate core. *Chem.—Eur. J.* **2011**, *17*, 10029−10038. (b) Schierholt, A.; Hartmann, M.; Lindhorst, T. K. Bi- and trivalent glycopeptide mannopyranosides as inhibitors of type 1 fimbriae-mediated bacterial adhesion: variation of valency, aglycon and scaffolding. *Carbohydr. Res.* **2011**, *346*, 1519−1526. (c) Schierholt, A.; Hartmann, M.; Schwekendiek, K.; Lindhorst, T. K. Cysteine-based mannoside glycoclusters: synthetic routes and antiadhesive properties. *Eur. J. Org. Chem.* **2010**, 3120−3128. (d) Gouin, S. G.; Wellens, A.; Bouckaert, J.; Kovensky, J. Synthetic multimeric heptyl mannosides as potent antiadhesives of uropathogenic *Escherichia coli*. *ChemMedChem* **2009**, *4*, 749−755. (e) Touaibia, M.; Wellens, A.; Shiao, T. C.; Wang, Q.; Sirois, S.; Bouckaert, J.; Roy, R. Mannosylated G(0) dendrimers with nanomolar affinities to *Escherichia coli* FimH. *ChemMedChem* **2007**, *2*, 1190−1201. (f) Touaibia, M.; Shiao, T. C.; Papadopoulos, A.; Vaucher, J.; Wang, Q. G.; Benhamioud, K.; Roy, R. Tri- and hexavalent mannoside clusters as potential inhibitors of type 1 fimbriated bacteria using pentaerythritol and triazole linkages. *Chem. Commun.* **2007**, 380−382. (g) Touaibia, M.; Roy, R. Glycodendrimers as anti-adhesion drugs against type 1 fimbriated *E. coli* uropathogenic infections. *Mini-Rev. Med. Chem.* **2007**, *7*, 1270−1283. (h) Nagahori, N.; Lee, R. T.; Nishimura, S.; Page, D.; Roy, R.; Lee, Y. C. Inhibition of adhesion of type 1 fimbriated *Escherichia coli* to highly mannosylated ligands. *ChemBioChem* **2002**, *3*, 836−844. (i) Furneaux, R. H.; Pakulski, Z.; Tyler, P. C. New mannotriosides and trimannosides as potential ligands for mannose-specific binding proteins. *Can. J. Chem.* **2002**, *80*, 964−972. (j) Lindhorst, T. K.; Kieburg, C.; Krallmann-Wenzel, U. Inhibition of the type 1 fimbriae-mediated adhesion of *Escherichia coli* to erythrocytes by multiantennary alpha-mannosyl clusters: the effect of multivalency. *Glycoconjugate J.* **1998**, *15*, 605−613. (k) Kotter, S.; Krallmann-Wenzel, U.; Ehlers, S.; Lindhorst, T. K. Multivalent ligands for the mannose-specific lectin on type 1 fimbriae of *Escherichia coli*: syntheses and testing of trivalent alpha-D-mannoside clusters. *J. Chem. Soc., Perkin Trans. 1* **1998**, 2193−2200. (l) Dubber, M.; Sperling, O.; Lindhorst, T. K. Oligomannoside mimetics by glycosylation of "octopus glycosides" and their investigation as inhibitors of type 1 fimbriae-mediated adhesion of *Escherichia coli*. *Org. Biomol. Chem.* **2006**, *4*, 3901−3912. (m) Papadopoulos, A.; Shiao, T. C.; Roy, R. Diazo transfer and click chemistry in the solid phase syntheses of lysine-based glycodendrimers as antagonists against *Escherichia coli* FimH. *Mol. Pharmaceutics* **2012**, *9*, 394−403.

(21) Hung, C. S.; Bouckaert, J.; Hung, D.; Pinkner, J.; Widberg, C.; DeFusco, A.; Auguste, C. G.; Strouse, R.; Langermann, S.; Waksman, G.; Hultgren, S. J. Structural basis of tropism of *Escherichia coli* to the bladder during urinary tract infection. *Mol. Microbiol.* **2002**, *44*, 903−915.

(22) Bouckaert, J.; Berglund, J.; Schembri, M.; de Genst, E.; Cools, L.; Wuhrer, M.; Hung, C.-S.; Pinkner, J.; Slattegard, R.; Zavialov, A.; Choudhury, D.; Langermann, S.; Hultgren, S. J.; Wyns, L.; Klemm, P.; Oscarson, S.; Knight, S. D.; De Greve, H. Receptor binding studies disclose a novel class of high-affinity inhibitors of the *Escherichia coli* FimH adhesion. *Mol. Microbiol.* **2005**, *55*, 441−455.

(23) Wellens, A.; Garofalo, C.; Nguyen, H.; Van Gerven, N.; Slattegård, R.; Hernalsteens, J. P.; Wyns, L.; Oscarson, S.; De Greve, H.; Hultgren, S.; Bouckaert, J. Intervening with urinary tract infections using antiadhesives based on the crystal structure of the FimH-oligomannose-3 complex. *PLoS One* **2008**, *3*, e2040.

(24) Sperling, O.; Fuchs, A.; Lindhorst, T. K. Evaluation of the carbohydrate recognition domain of the bacterial adhesin FimH: design, synthesis and binding properties of mannoside ligands. *Org. Biomol. Chem.* **2006**, *4*, 3913−3922.

(25) Han, Z.; Pinkner, J. S.; Ford, B.; Obermann, R.; Nolan, W.; Wildman, S. A.; Hobbs, D.; Ellenberger, T.; Cusumano, C. K.; Hultgren, S. J.; Janetka, J. W. Structure-based drug design and optimization of mannoside bacterial fimH antagonists. *J. Med. Chem.* **2010**, *53*, 4779−4792.

(26) Klein, T.; Abgottspon, D.; Wittwer, M.; Rabbani, S.; Herold, J.; Jiang, X.; Kleeb, S.; Lüthi, C.; Scharenberg, M.; Bezençon, J.; Gubler, E.; Pang, L.; Smiesko, M.; Cutting, B.; Schwardt, O.; Ernst, B. FimH antagonists for the oral treatment of urinary tract infections: from design and synthesis to in vitro and in vivo evaluation. *J. Med. Chem.* **2010**, *53*, 8627−8641.

(27) (a) Gupta, K; Hooton, T. M.; Stamm, W. E. Increasing antimicrobial resistance and the management of uncomplicated community-acquired urinary tract infections. *Ann. Intern. Med.* **2001**, *135*, 41−50. (b) Blango, M. G.; Mulvey, M. A. Persistence of uropathogenic *Escherichia coli* in the face of multiple antibiotics. *Antimicrob. Agents Chemother.* **2010**, *54*, 1855−1863.

(28) Hultgren, S. J.; Schwan, W. R.; Schaeffer, A. J.; Duncan, J. L. Regulation of production of type 1 pili among urinary tract isolates of *Escherichia coli*. *Infect. Immun.* **1986**, *54*, 613−620.

(29) Ren, D.; Zuo, R.; Barrios, A. F. G.; Bedzyk, L. A.; Eldridge, G. R.; Pasmore, M. E.; Wood, T. K. Differential gene expression for investigation of *Escherichia coli* biofilm inhibition by plant extract ursolic acid. *Appl. Environ. Microbiol.* **2005**, *71*, 4022−4034.

(30) France, R. R.; Compton, R. G.; Davis, B. G.; Fairbanks, A. J.; Rees, N. V.; Wadhawan, J. D. Selective electrochemical glycosylation by reactivity tuning. *Org. Biomol. Chem.* **2004**, *2*, 2195−2202.

(31) (a) Ishiyama, T.; Murata, M.; Miyaura, N. Palladium(0)-catalyzed cross-coupling reaction of alkoxydiboron with haloarenes: a direct procedure for arylboronic esters. *J. Org. Chem.* **1995**, *60*, 7508−7510. (b) Takagi, J.; Takahashi, K.; Ishiyama, T.; Miyaura, N. Palladium-catalyzed cross-coupling reaction of bis(pinacolato)diboron with 1-alkenyl halides or triflates: convenient synthesis of unsymmetrical 1,3-dienes via the borylation-coupling sequence. *J. Am. Chem. Soc.* **2002**, *124*, 8001−8006. (c) Thompson, A. L. S.; Kabalka, G. W.; Akula, M. R.; Huffman, J. W. The conversion of phenols to the corresponding aryl halides under mild conditions. *Synthesis* **2005**, 547−550.

(32) Schwizer, D.; Gäthje, H.; Kelm, S.; Porro, M.; Schwardt, O.; Ernst, B. Antagonists of the myelin-associated glycoprotein: a new class of tetrasaccharide mimics. *Bioorg. Med. Chem.* **2006**, *14*, 4944−4957.

(33) (a) Ashwell, S.; Gero, T.; Ioannidis, S.; Janetka, J.; Lyne, P.; Su, M.; Toader, D.; Yu, D.; Yu, Y. Preparation of Substituted Heterocycles, Particularly Ureidothiophenes, as CHK1 Kinase Inhibitors for Treating Neoplasm. PCT Int. Appl. WO 2005066163, 2005. (b) Janetka, J. W.; Almeida, L.; Ashwell, S.; Brassil, P. J.; Daly, K.; Deng, C.; Gero, T.; Glynn, R. E.; Horn, C. L.; Ioannidis, S.; Lyne, P.; Newcombe, N. J.; Oza, V. B.; Pass, M.; Springer, S. K.; Su, M.; Toader, D.; Vasbinder, M. M.; Yu, D.; Yu, Y.; Zabludoff, S. D. Discovery of a novel class of 2-ureido thiophene carboxamide checkpoint kinase inhibitors. *Bioorg. Med. Chem. Lett.* **2008**, *18*, 4242−4248.

(34) Niesen, F.; Berglund, H.; Vedadi, M. The use of differential scanning fluorimetry to detect ligand interactions that promote protein stability. *Nat. Protoc.* **2007**, *2*, 2212−2221.

(35) Kranz, J. K.; Schalk-Hihi, C. Protein thermal shifts to identify low molecular weight fragments. *Methods Enzymol.* **2011**, *493*, 277−298.

(36) Cusumano, C. K.; Pinkner, J. S.; Han, Z.; Greene, S. E.; Ford, B. A.; Crowley, J. R.; Henderson, J. P.; Janetka, J. W.; Hultgren, S. J. Treatment and prevention of urinary tract infection with orally active FimH inhibitors. *Sci. Transl. Med.* **2011**, *3*, 109ra115.
(37) Ernst, B.; Magnani, J. L. From carbohydrate leads to glycomimetic drugs. *Nat. Rev. Drug Discovery* **2009**, *8*, 661−677.
(38) (a) Kansy, M.; Senner, F.; Gubernator, K. Physicochemical high throughput screening: parallel artificial membrane permeation assay in the description of passive absorption processes. *J. Med. Chem.* **1998**, *41*, 1007−1010. (b) Avdeef, A.; Bendels, S.; Di, L.; Faller, B.; Kansy, M.; Sugano, K.; Yamauchi, Y. Parallel artificial membrane permeability assay (PAMPA)-critical factors for better predictions of absorption. *J. Pharm. Sci.* **2007**, *96*, 2893−2909.
(39) Schwardt, O.; Rabbani, S.; Hartmann, M.; Abgottspon, D.; Wittwer, M.; Kleeb, S.; Zalewski, A.; Smieško, M.; Cutting, B.; Ernst, B. Design, synthesis and biological evaluation of mannosyl triazoles as FimH antagonists. *Bioorg. Med. Chem.* **2011**, *19*, 6454−6473.